Chapter 6
Parametric analysis of asphalt pavements

6.1 Introduction

In India, the guidelines for the analytical design of asphalt concrete pavement proposes the use of layered elastic theory. The program IITPAVE [20] is commonly used to calculate stress, strain, and displacements at critical locations within the pavement structure. Due to its simplicity, layered elastic theory has been utilized by pavement engineers for several decades. The advancement in research and experimental knowledge has expanded the arc of layered elastic theory to handle complex material properties like viscoelasticity and nonlinearity. However, the features of software program like IITPAVE [20] based on layered elastic theory is still limited. It assumes each layer as linear elastic, homogeneous, and isotropic. All the layers are considered infinite in lateral extent and have a finite thickness except for the subgrade layer, which is assumed to be infinite. The pavement surface is loaded uniformly and statically over a circular area. However, in reality, the complex asphalt pavement system may be very different than assumptions made in IITPAVE [20].

Generally, the lateral extents of pavement layers are finite, material properties are not linear elastic, and loading conditions are nonuniform. These differences may result in significant deviations between the calculated and actual field response of asphalt pavement system. So, there is need to adopt suitable analysis techniques which can consider these complexities to reach at a more comprehensive and realistic design procedures.

The finite element (FE) method, a numerical analysis technique used for obtaining approximate solutions to a numerous types of engineering problems, these specific requirements can be met and the response of asphalt pavement can be determined more realistically. The objective of this study was to develop a 3-dimensional FE model of tire-pavement system that would predict the mechanistic response of asphalt pavement under overloading and extreme high temperature conditions. Overloading has been reported as one of the major concerns for increasing pavement damage in India. So, effect of overloading on the structural response and pavement life has been studied. Since, India is a country of tropical climate and peak temperature during summer is continuously increasing. Although it doesn't last long but poses serious concern for asphalt mix stiffness. Thus, study of temperature effect on pavement response was realized. Since, overloading and increase in temperature results in structural loss of pavement, remedial measures in terms of effect of stabilization methods and increase in layer thicknesses to control critical strains were also studied.

Although, present study aims to evaluate viscoelastic response of asphalt pavement considering stress dependent behaviour of UGMs and nonuniform loading conditions, analysis was also done considering linear elastic theory and uniform loading condition as being currently practiced. This will help in understanding the quantitative deviation in the results obtained from the two approaches. For this purpose, the entire study has been divided in four stages of FE simulation. The first stage of simulation considers linear elastic material properties of various layers and uniform loading condition, the second stage of simulation considers linear elastic material properties and nonuniform loading conditions using real tire. These two analyses can capture the effect of nonuniform contact stress distribution at tire pavement interface. The third stage of simulation considers LVE response of asphalt mixes and linear elastic properties of UGMs while last stage of

simulation considers LVE response of asphalt mixes and stress dependent behaviour of UGMs. The third and fourth stage of simulation considers nonuniform loading condition. The following sections briefly discusses results obtained from these stages of simulation.

6.1.1 Stage I: Linear elastic materials and uniform loading

The first stage of simulation deals with the basic layered elastic approach in which load is applied uniformly at the pavement surface. This simulation will create a reference data set as per the considerations of current pavement analysis and design guidelines. In later part of the simulations, gradually material complexities and environmental conditions using nonuniform loading to simulate a more realistic field condition will be considered.

In this stage, all the layers are assumed as linear elastic and material properties of asphalt concrete layer is based on resilient modulus test while unbound granular layers are based on soaked CBR test. Empirical relations as specified in IRC:37 (see Eq. 6.1-6.3) has been used to evaluate resilient modulus of these layers based on CBR values.

$$M_{RS} = 10 \times CBR \qquad for\ CBR \leq 5\% \tag{6.1}$$

$$M_{RS} = 17.6 \times (CBR)^{0.64} \qquad for\ CBR > 5\% \tag{6.2}$$

$$M_{RGRAN} = 0.2 \times (h)^{0.45} \times M_{RSUPPORT} \tag{6.3}$$

where, M_{RS} is resilient modulus of subgrade soil (in MPa), CBR is California bearing ratio of subgrade soil (%), M_{RGRAN} is resilient modulus of granular layers (the granular base and subbase layer are considered as single layer for the purpose of analysis and single modulus value is assigned to the combined layer), h is thickness of granular layer in mm, and $M_{RSUPPORT}$ is resilient modulus of the supporting layer (MPa).

In this stage of analysis, loading has been assumed uniform and different contact shapes (circular, square, rectangular, and rectangle with semi-circular ends) have been

considered for evaluating pavement response. These results will be compared later with the pavement response in case of nonuniform contact stress distribution (considering realistic solid tire body) to study relative accuracy of these loading shapes.

6.1.2 Stage II: Linear elastic materials and nonuniform loading

The second stage of the simulation focuses on considering loading nonuniformity based on layered elastic approach. In this stage, material properties of all the layers are considered linear elastic while a nonuniform contact stress distribution at tire-pavement interface is simulated using a realistic solid tire body. The effect of different tire loads (including over-loading), mixture type, temperature, and layer thicknesses on the structural response was analysed. The data obtained from these simulations were used for the relative comparisons. In the later part of this stage of the simulation, the base layer was replaced with the ETA layer to study the effect of emulsion-treated base layer stabilization on pavement responses. The goal of this study was to check if the ETA stabilization technique can help in the reduction of top-layer thickness without compromising pavement performance.

Since, rutting and fatigue is a common distress type, the performance of the pavement was evaluated considering these two. Subgrade rutting and AC fatigue life were calculated on the basis of empirical relations (Eq. 6.4-6.6) as specified by IRC [20] for 90% reliability.

$$N_R = 1.41 \times 10^{-8} \left(\frac{1}{\varepsilon_z}\right)^{4.5337} \tag{6.4}$$

where N_R is rutting life of subgrade (measured as cumulative equivalent number of 80 kN standard axle load served by pavement before the rut depth of 20 mm or more) and ε_z is the vertical compressive strain at the top of the subgrade layer.

$$N_f = 0.5161 \times C \times 10^{-4} \left(\frac{1}{\varepsilon_t}\right)^{3.89} \times \left(\frac{1}{M_r}\right)^{0.854} \quad (6.5)$$

$$C = 10^M \; and \; M = 4.84\left(\frac{V_{be}}{V_a + V_{be}} - 0.69\right) \quad (6.6)$$

where N_f is fatigue life of asphalt layer (cumulative equivalent number of 80 kN standard axle load served by pavement before the critical cracked area of 20% or more), V_{be} is percent volume of effective binder in the mix, V_a is air void in the mix (%), ε_t is the horizontal tensile strain at the bottom of AC layer, and M_r is the resilient modulus of the AC mix. N_R and N_f have been evaluated in millions of standard axle (msa) load repetitions.

6.1.3 Stage III: LVE AC, elastic UGMs and nonuniform loading

The third stage of simulation studies effect of various parameters on the structural response and pavement life considering linear viscoelastic properties of asphalt mixes (BC-2) and linear elastic properties of unbound granular layers. The nonuniform contact stress distribution at tire-pavement interface using a realistic solid tire body has been considered in the analysis for pavement loading. This analysis will help in understanding pavement engineers, whether pavement strength and hence its life is underestimated or overestimated using linear elastic properties being currently practiced in India.

6.1.4 Stage IV: LVE AC, stress dependent UGMs and nonuniform loading

The last stage of simulation deals with linear viscoelastic properties of asphalt mixes and nonlinear stress dependent material behaviour of unbound granular layers. The stress dependent resilient modulus of base and subbase layers have been evaluated using k-θ model, Uzan model, and NCHRP model while for subgrade layer Bilinear model has been

used as discussed in chapter 5. The loading condition has been kept similar as in the previous stage of the simulation (nonuniform using realistic tire body). The results of this stage of simulation will be further compared with stage II analysis so that difference in estimating pavement response and its life using the two approaches can be assessed. It will help in understanding the role of material characterization and choice of loading in pavement analysis and design.

6.2 Linear elastic material properties and uniform loading

This stage of simulation considers linear elastic properties of various layers of the asphalt pavement. All the analysis methods (analytical or numerical) commonly use elastic/resilient modulus and Poisson's ratio of the materials as an input parameter. So, for our FE analysis, resilient modulus of asphalt layer was obtained using resilient modulus test as discussed in Chapter 4 while resilient modulus of unbound granular layers was obtained using empirical relations based on soaked CBR values. Poisson's ratio of the materials has not been determined experimentally and have been directly used as per the specifications of IRC:37 for various layers. Input parameters of the FE model (see Figure 3.5) such as M_r and υ of the unbound granular layers and asphalt concrete layer (BC-2 used as top layer) is given in Table 6.1. The loading conditions were assumed uniform and static in the first stage of analysis and various contact shapes (circular, square, rectangular, and rectangular with semi-circular ends) as shown in Figure 6.1 were considered. Currently, circular loading area is considered in pavement analysis using IITPAVE software, so the idea was to study if different contact shapes impact pavement response significantly or not.

Table 6.1. Material properties (linear elastic) of pavement layers

S No.	Pavement layers	Thickness	CBR (%)	M_r (MPa)	υ
1	Subgrade	500	10.80	80	0.35
2	Subbase	350	N. A	295	0.35
3	Base (WMM)	300	N. A	295	0.35
4	Asphalt concrete	150	N. A	3373	0.35

The analysis was done considering 80 kN of standard single axle load and 0.56 MPa of tire pressure on the pavement surface as specified in IRC:37. For simplicity in analysis, single tire load of 40 kN (equally distributed both side) was considered in the analysis. The FE model of asphalt pavement system (see Figure 3.4), boundary conditions, element types, and model related other details can be found in section 3.4.

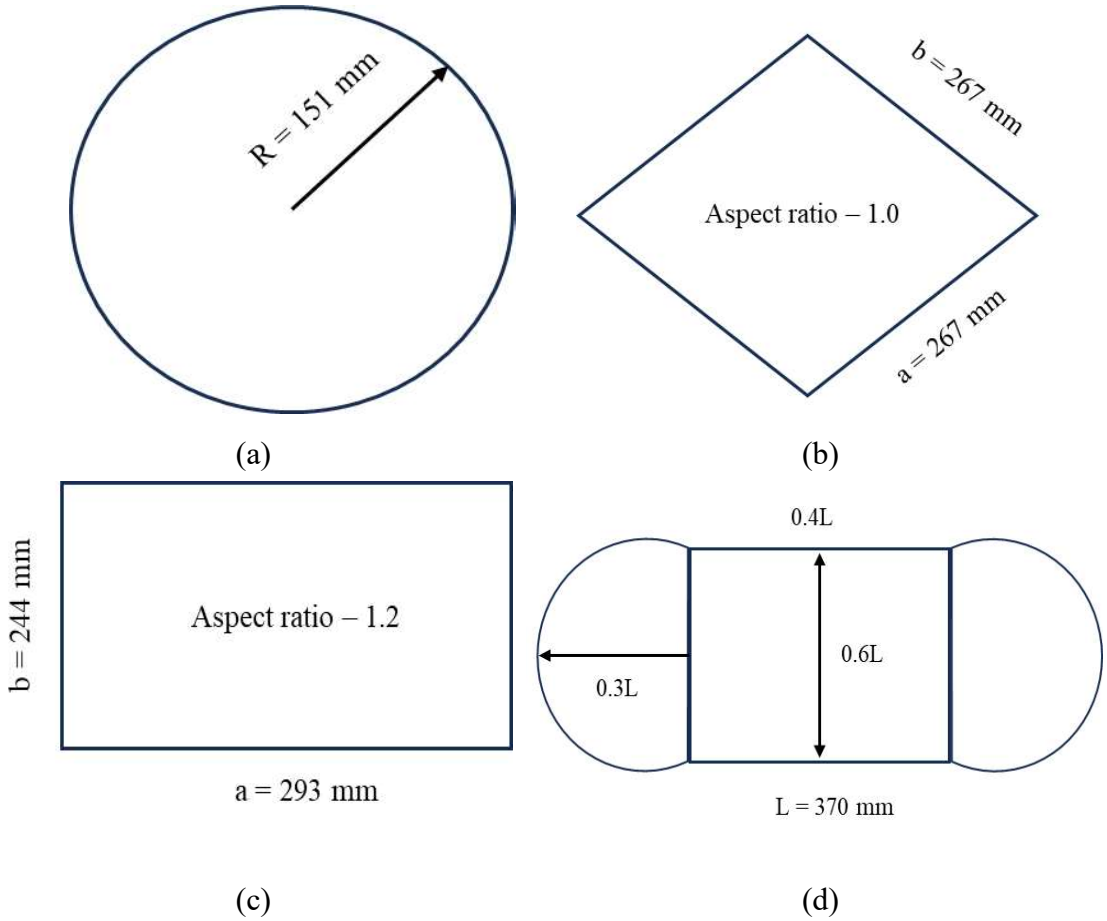

Figure 6.1. The assumed shape of tire loading (a) circular (b) square (c) rectangular and (d) rectangle with semi-circular ends.

The aspect ratio is defined as the ratio of length to width of the particular loading shape. So, for square loading it is 1 while for rectangular loading a trial aspect ratio of 1.2 has been chosen. The area and thus dimensions of a particular shape of tire loading are based on magnitude and pressure on loaded area. The effect of loading shapes on the structural response (maximum deformation and normal strain) of asphalt pavement has been shown in Figure 6.2.

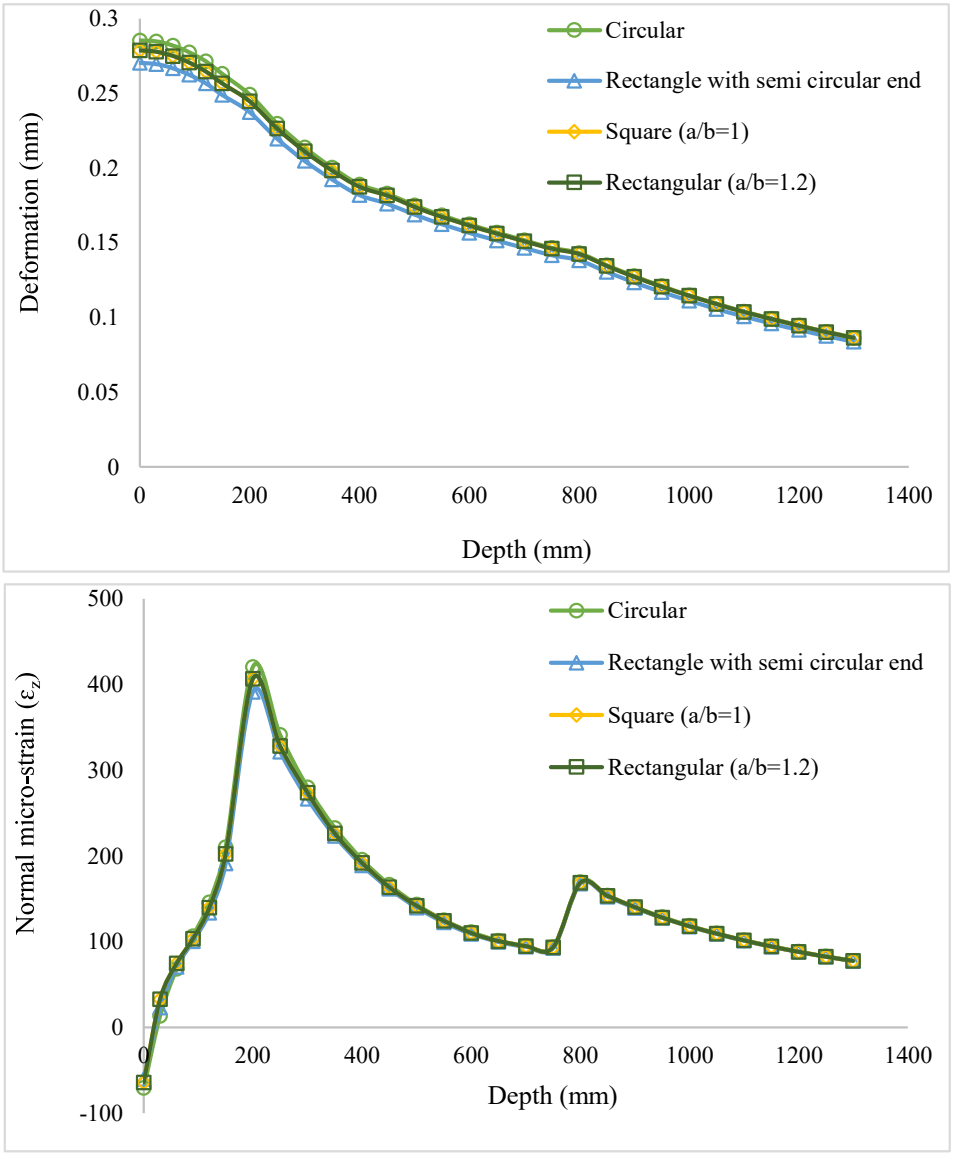

Figure 6.2. Effect of loading shapes on structural response of asphalt pavement.

As shown in Figure 6.2, there was no significant difference in structural response found due to change in various loading shapes. It was found that, the tire contact shape, rectangle

with semi-circular ends results in lowest pavement response while circular shape gives highest pavement response. Square (aspect ratio-1.0) and rectangular shape (aspect ratio-1.2) gives similar results. The average difference in maximum deformation using circular and rectangle with semi-circular shape was found to be 4.07% while this difference for normal strain was found to be 3.30% only. The effect of square and rectangular (aspect ratio-1.2) loaded area on the deformation and normal strain was found somewhere in between as that of circular and rectangle with semi-circular loaded area.

In this study, not much difference in the mechanistic response of asphalt pavement was found due to change in the shape of loading area. The parametric study for this stage of simulation has not been presented as the idea of this analysis was to study if there is any significant difference in structural response of the asphalt pavement considering different assumed loading shapes. The variation of deformation and normal strain with pavement depth will be explained in next section when parametric studies are presented.

6.3 Linear elastic materials and nonuniform loading

Stage II simulation considers linear elastic material properties of all the pavement layers as evaluated and reported in Table 6.1. However, a three-dimensional FE model of solid tire (see Figure 3.4) has been used in this simulation to study the effect of nonuniform contact stress distribution at tire-pavement interface. Parametric studies considering effect of various parameters (loading, asphalt mixes, temperature, layer thickness, and base layer stabilization) on the structural response and pavement life has been studied and presented.

6.3.1 Effect of load on the structural response of AC pavement

The maximum permissible weight in India for single axle with two tires is 7.5 tonnes (75 kN) as per the guidelines of MoRTH [216] notification, 2018. However, the standard axle

load considered for pavement analyses as per IRC [20] recommendations is 80 kN. For simplicity in analysis, the load can be considered as evenly distributed, hence, half of the loads (40 kN) were considered on either side of the axle as shown in Figure 6.3.

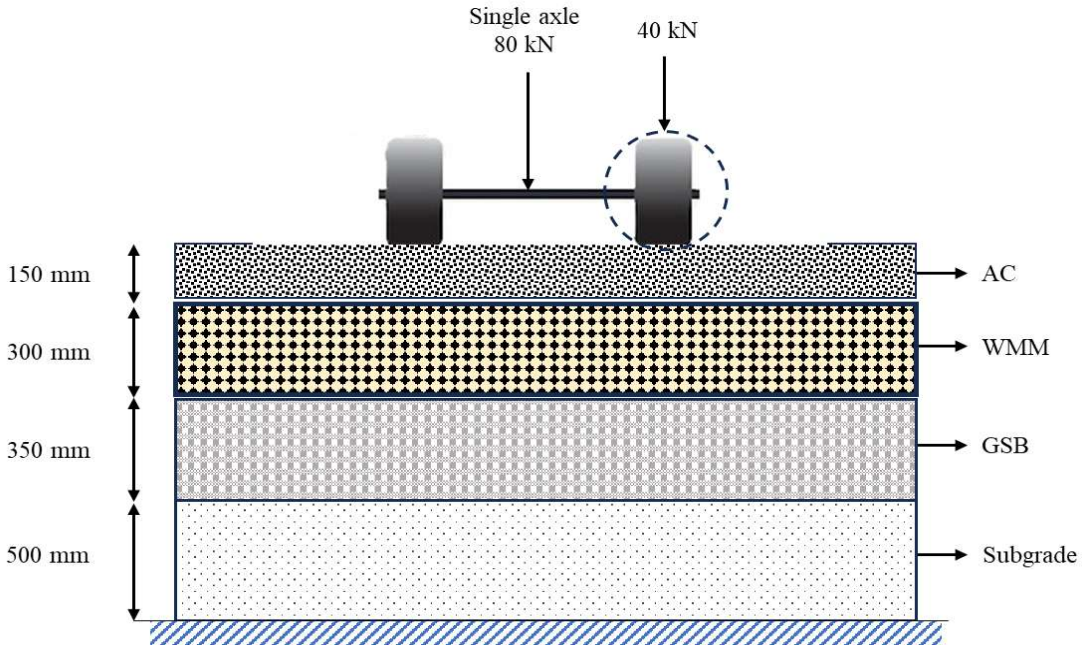

Figure 6.3. Pavement structure and loading configuration.

Load beyond the permissible legal limit is considered as overloading and it has been a major challenge in many of the developing nations including India. It was found that an AC pavement which is generally designed for 15 years when subjected to 5% of overloading, the design life is reduced by 2.7 years [267]. So, it is important to study the effect of overloading on the structural response of asphalt pavement. The reduction in pavement life in rutting and fatigue has also been evaluated as shown in Table 6.2.

The effect of an increase in axle loading on pavement responses, vertical deformation, ε_z, ε_t, σ_z, and σ_t are shown in Figure 6.4(a)-(f) respectively. The vertical compressive stress (σ_z) and tensile stress (σ_t) were evaluated at z =150 mm.

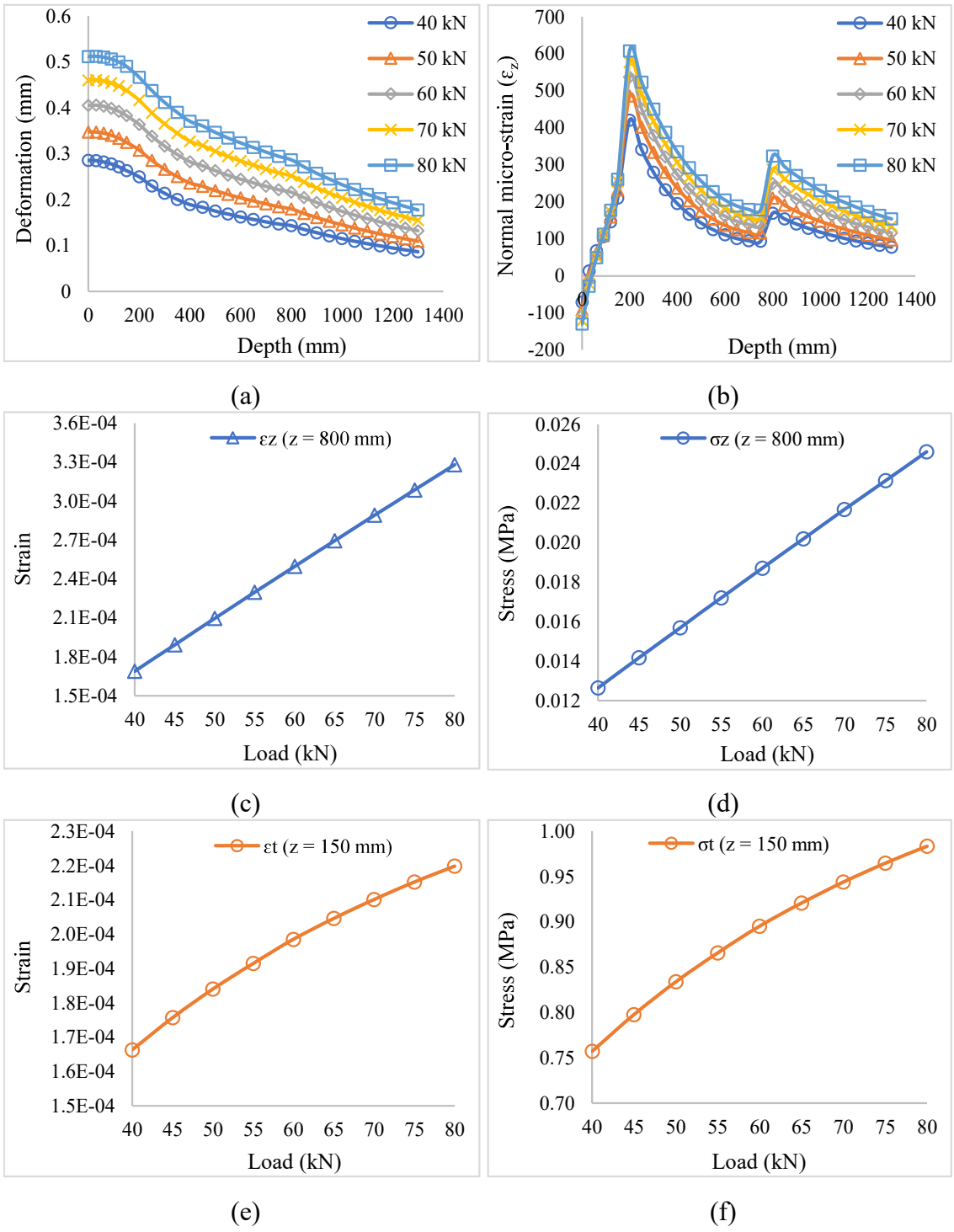

Figure 6.4. Effect of axle loading on pavement response.

As shown in Figure 6.4 (a), the vertical deformation decreases with an increase in the pavement depth and increases with an increase in the tire load. Maximum vertical deformation is observed at the pavement surface (directly below the tire load) as stress is highest at this point and gradually decreases with the pavement depth as stress disperses

to larger area. An overloading of 25% from design load of 40 kN on single tire to 50 kN results in an increase of 21.75% in vertical deformation in the AC layer (see Table 6.2). It was further observed that the effect of the increasing load is more significant in the upper layers of the pavement as the load is directly coming over the top surface and reduces significantly after the AC layer.

Since, the normal strains with depth under tire load, ε_z, and ε_t are important parameters and are used in pavement performance analysis, variations of these strains are shown in Figure 6.4 (b), (c), and (e) respectively. The normal strain is initially tensile up to a depth of about 40 mm due to bending stress in asphalt layer, gradually compressive strain starts building in the pavement layers. To make ease of understanding, the data of Figure 6.4 is presented in tabular form with their respective % changes in Table 6.2 and effect of overloading on rutting and fatigue life of the asphalt pavement is shown in Figure 6.5.

Table 6.2. Effect of loading on maximum deformation, strains, and pavement life

Load	**40 kN**	**50 kN**	**60 kN**	**70 kN**	**80 kN**
Maximum deformation	0.285	0.347	0.405	0.459	0.511
% increase in deformation		21.750	42.110	61.050	79.300
ε_z (micro-strains) at top of the	168.900	209.600	249.700	289.100	328.000
% increase in ε_z		24.100	47.840	71.170	94.200
ε_t (micro-strains) at the bottom	166.300	184.000	198.500	210.100	219.800
% increase in ε_t		10.640	19.360	26.340	32.170
Subgrade rutting life, msa (N_R)	1786.000	671.000	303.000	156.000	88.000
% reduction in rutting life		62.430	83.030	91.270	95.070
Fatigue life of AC layer, msa	58.000	39.000	29.000	23.000	19.000
% reduction in fatigue life		32.760	50.000	60.340	67.240

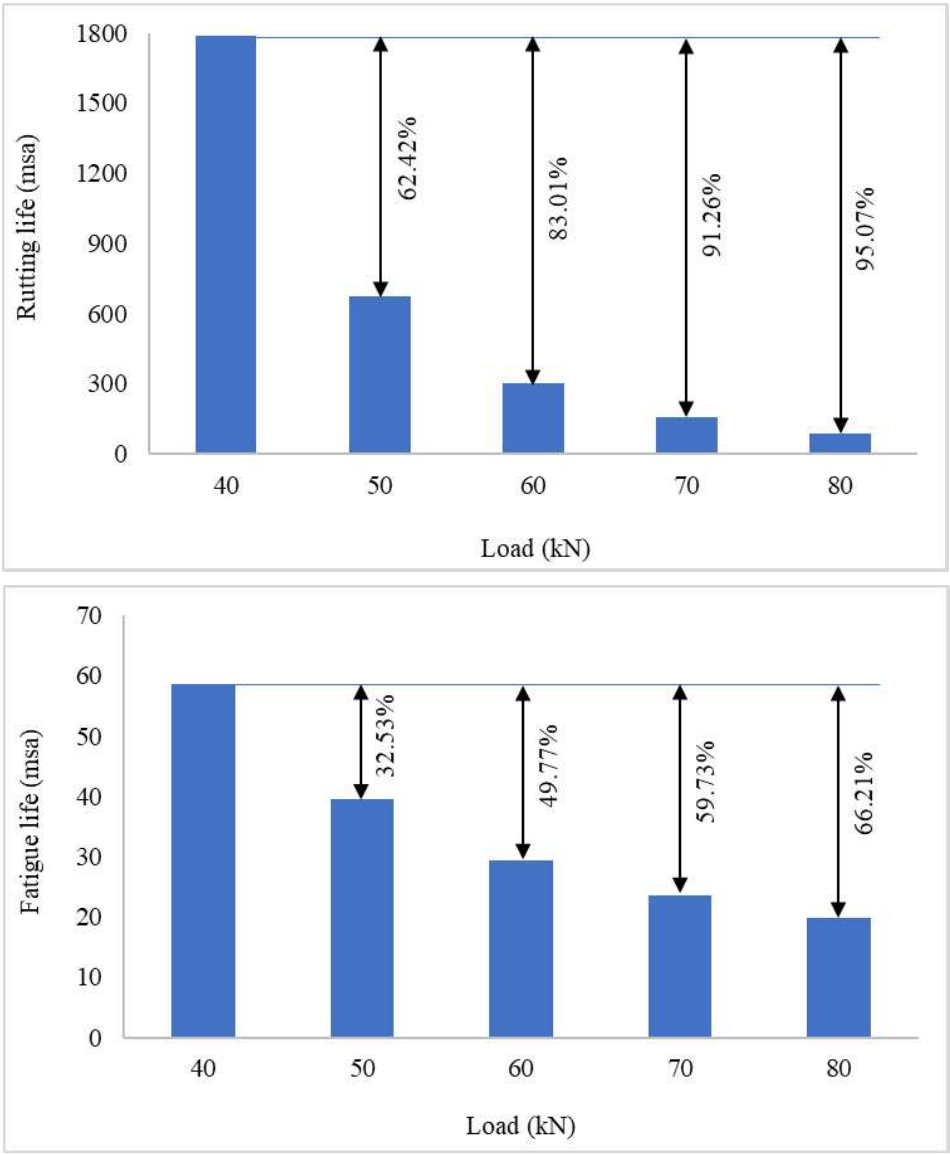

Figure 6.5. Effect of overloading on rutting and fatigue life.

In the asphalt concrete layer, normal strain shows an increasing trend, whereas it keeps on decreasing in the lower layers as stress decreases with the pavement depth. A sharp increase in the normal compressive strain near the interface of asphalt-base and subbase-subgrade layer was found as stiffness of the material reduces. The observed behaviour is similar to the findings of past research studies [268,269]. The normal compressive strain at the top the subgrade (ε_z at z = 800 mm) as shown in Figure 6.4 (c) was found to increase linearly with the increase in axle loading. However, the variation of tensile strain at the bottom of asphalt layer (ε_t at z = 150 mm) is not linear, instead it is a polynomial

(quadratic) fit. The effect of overloading is much more significant on ε_z compared to ε_t. An increase in loading from 40 kN to 50 kN, increases ε_z by 24.10% whereas ε_t increases by 10.64% with the same increase in loading.

Similarly, as shown in Figure 6.4 (d) and (f), the values of σ_z and σ_t at a depth of 800 mm and 150 mm were evaluated respectively. An increase of 24.13% in σ_z was observed for a change in load from 40 kN to 50 kN, however, σ_t was found to increase by 10.15% for the same change in vertical loading.

As shown in Figure 6.5 as well as Table 6.2, an increase in load significantly reduces the subgrade rutting (N_R) and fatigue life (N_f) of AC layer of the pavement. For example, an overloading of 10 kN (25%) from 40 kN to 50 kN, reduces the rutting life of the subgrade layer by 62.43% and fatigue life of the AC layer by 32.76%. From the above observations, it can be clearly seen that the developed FE model can appropriately capture the pavement response behaviour.

6.3.2 Effect of mix type and temperature

In line with the objective of the study, the effect of temperature on pavement responses at different temperatures was studied considering conventional base layer. The composition of pavement and material properties of UGMs are same as outlined in Figure 6.3 and Table 6.1 respectively. In India, the average annual temperature falls near 25 ^oC and reaches to 45 ^oC in summer, so a temperature range of 25 ^oC to 45 ^oC was considered. Effect of temperature on M_r values of AC mixes (BC-1, BC-2, SMA-1, and SMA-2) was evaluated and same has been considered to analyze its effect on the structural response of the pavement. Pavement responses in terms of vertical deformation and ε_z were studied for all the mixtures, as shown in Figure 6.6(a)-(h).

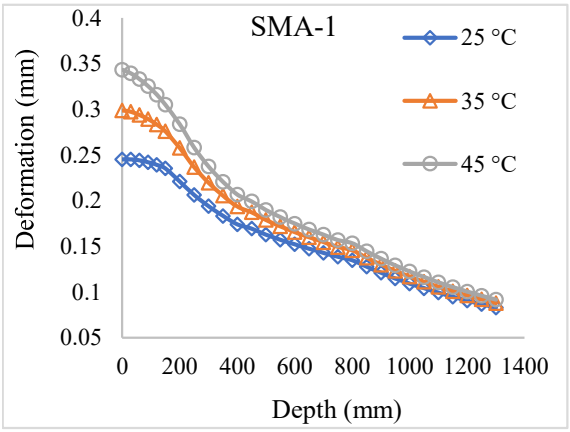
SMA-1
25 °C
35 °C
45 °C
Deformation (mm)
0.4
0.35
0.3
0.25
0.2
0.15
0.1
0.05
0
200
400
600
800
1000
1200
1400
Depth (mm)

(a)

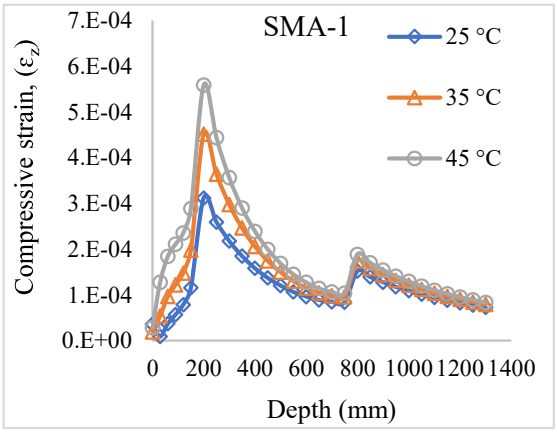
SMA-1
25 °C
35 °C
45 °C
Compressive strain, (ε_z)
7.E-04
6.E-04
5.E-04
4.E-04
3.E-04
2.E-04
1.E-04
0.E+00
0
200
400
600
800
1000
1200
1400
Depth (mm)

(e)

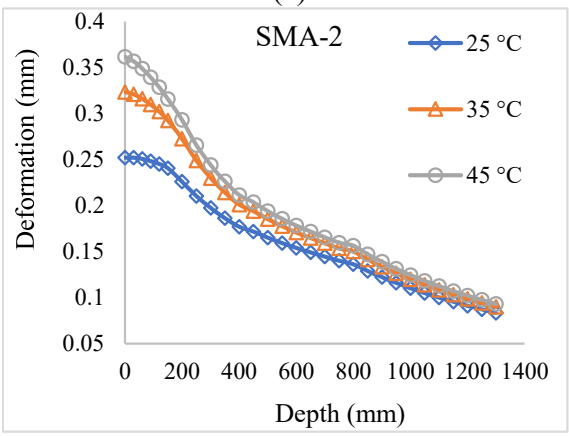
SMA-2
25 °C
35 °C
45 °C
Deformation (mm)
0.4
0.35
0.3
0.25
0.2
0.15
0.1
0.05
0
200
400
600
800
1000
1200
1400
Depth (mm)

(b)

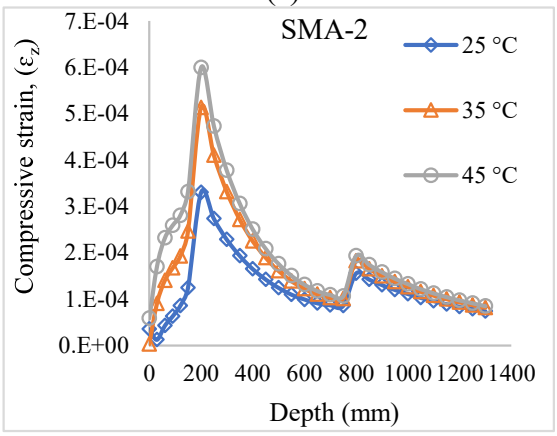
SMA-2
25 °C
35 °C
45 °C
Compressive strain, (ε_z)
7.E-04
6.E-04
5.E-04
4.E-04
3.E-04
2.E-04
1.E-04
0.E+00
0
200
400
600
800
1000
1200
1400
Depth (mm)

(f)

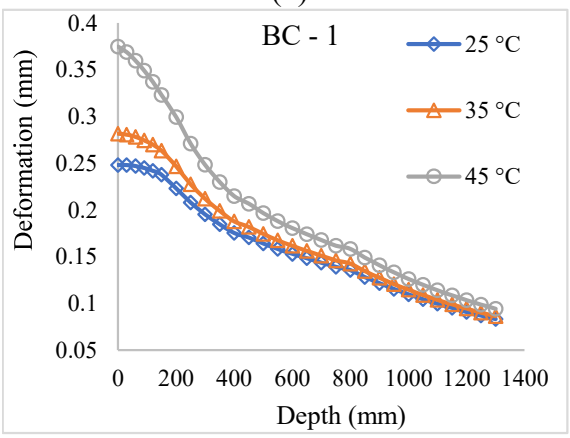
BC - 1
25 °C
35 °C
45 °C
Deformation (mm)
0.4
0.35
0.3
0.25
0.2
0.15
0.1
0.05
0
200
400
600
800
1000
1200
1400
Depth (mm)

(c)

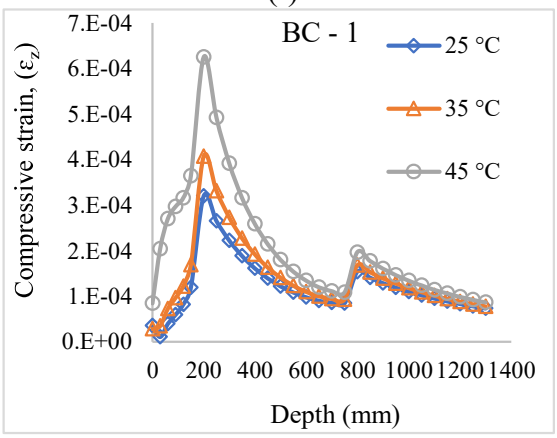
BC - 1
25 °C
35 °C
45 °C
Compressive strain, (ε_z)
7.E-04
6.E-04
5.E-04
4.E-04
3.E-04
2.E-04
1.E-04
0.E+00
0
200
400
600
800
1000
1200
1400
Depth (mm)

(g)

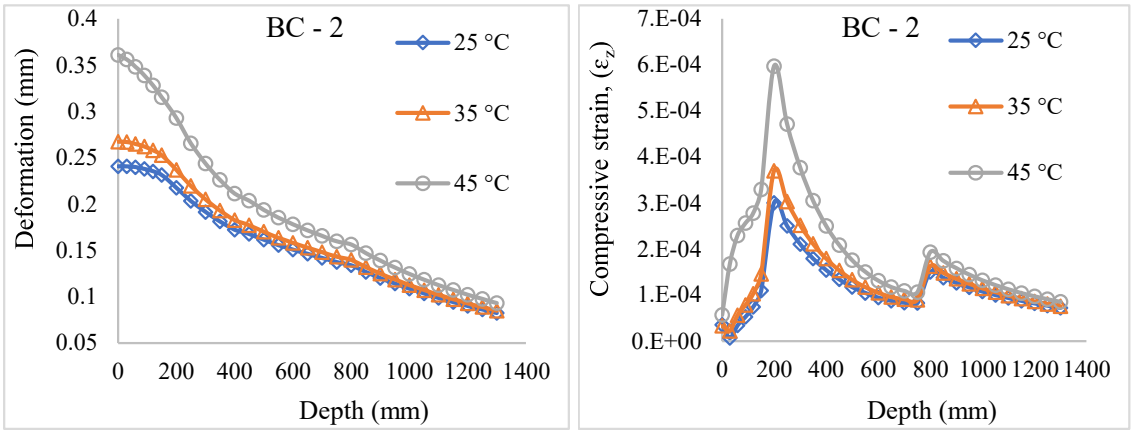

(d) (h)

Figure 6.6. Effect of mixes at different temperatures on deformation and ε_z at 40 kN.

As expected, figures (Figure 6.6 a-h) show that asphalt layer prepared with different mixes results in significantly different structural responses under same loading conditions.

Table 6.3. Effect of AC mixes and temperature on the pavement response

Mix type	Temp (°C)	Max. def in AC layer (mm)	% increase	ε_z (z = 800 mm) microstrains	% increase	N_R (msa)
SMA-1	25	0.245	N.A	152.20	N.A	2864
	35	0.298	21.63	174.20	14.45	1553
	45	0.343	15.10	188.20	08.04	1094
SMA-2	25	0.252	N.A	155.50	N.A	2599
	35	0.323	28.17	182.40	17.30	1261
	45	0.362	12.07	193.20	05.92	971
BC-1	25	0.248	N.A	153.60	N.A	2748
	35	0.281	13.30	167.90	09.31	1835
	45	0.375	33.45	196.50	17.03	900
BC-2	25	0.241	N.A	149.90	N.A	3069
	35	0.267	10.79	162.10	08.14	2152
	45	0.361	35.20	193.00	19.06	976

N.A – Not applicable.

As shown in Figure6.6, it was found that, the pavement response is sensitive to the mixture temperature. It was found that, at lower temperatures (25 and 35 ^{o}C), BC mixes are less sensitive to change in pavement response as compared to SMA mixes. However, at higher temperatures, material properties of BC mixes are more sensitive to change in temperature as compared to SMA mixes which leads to significant increase in pavement deformation and ε_z. As shown in Figure 6.6, change in maximum deformation and ε_z is higher for BC mixes than SMA mixes at higher temperatures. On the basis of data obtained from Figure 6.6, Table 6.3 was prepared to compare the relative performances of the mixture.

As shown in Table 6.3, at higher temperatures, the percentage change in vertical deformation in the AC layer and ε_z is found to be higher for BC samples than the SMA samples which implies that the effect of temperature was also found to be more prominent on BC mixes as compared to SMA mixes. For example, maximum deformation in the AC layer was found to increase by 33.45% and 35.20% for BC-1 and BC-2 mixes respectively when temperature increases from 35 to 45 ^{o}C. However, for the same change in temperature, the increase for SMA-1 and SMA-2 mixes are found to be 15.10% and 12.07% respectively. This could be explained by the fact that at lower temperatures, binder is stiff in the mix and BC offers more resistance to applied load due to relatively denser gradation. However, at the higher temperature, viscosity of binder reduces significantly, and load is mainly resisted by the aggregate skeleton. Since, SMA mixes are composed of a higher fraction of coarser particles, aggregate-to-aggregate contact is more effective. It is important to note that, for a change in temperature of 10 ^{o}C from 35 ^{o}C to 45 ^{o}C, rutting life of subgrade in case of BC mixes reduces significantly (52.80%) as compared to SMA mixes (26.27%). These findings support the usage of SMA mixes at extreme pavement temperatures where relatively higher deformations are expected. To

understand the effect of temperature on the rut response of the AC mix, material properties (M_r) at extreme pavement temperatures were evaluated, which will be discussed in the following paragraph.

In the current design guidelines, it is recommended that grades suitable for temperatures nearest to the specified maximum should be adopted [20]. The maximum pavement temperature prevailing in different parts of India together with suggested M_r values for BC-2 mixes are shown in Table 6.4.

Table 6.4. Pavement life subjected to maximum temperature [235] in various regions of India

City	State	Air temp (°C)	Pavement temp (°C)	Region	M_r (MPa)	N_R, msa	N_f, msa
Delhi	Delhi	45	66.87	North	339	542	34
Srinagar	J&K	28	50.74		727	788	25
Phalodi	Rajasthan	51	73.00		224	453	48
Surajpur	Chhattisgarh	46	68.30	Central	304	516	37
Munger	Bihar	47	69.11	East	288	505	38
Jalpaiguri	West Bengal	34	56.60		582	704	26
Guwahati	Assam	45	67.13		328	533	35
Mumbai	Maharashtra	35	57.93	West	542	679	27
Himmatnaga	Gujarat	42	64.46		388	577	31
Tirumangala	Tamil Nadu	40	62.26	South	438	611	29
Udupi	Karnataka	37	59.68		495	648	28
Vizianagara	A.P	48	70.34		264	486	41

Though these temperatures do not last long, they may play a vital role in the selection of suitable binder and deciding mix performance during their lifetime. Figure 6.7 presents the effect of maximum pavement temperature as experienced for various cities in India

on ε_z at the top of the subgrade layer, ε_t at the bottom of the AC layer, and maximum vertical deformation in the AC layer considering BC-2 mixes.

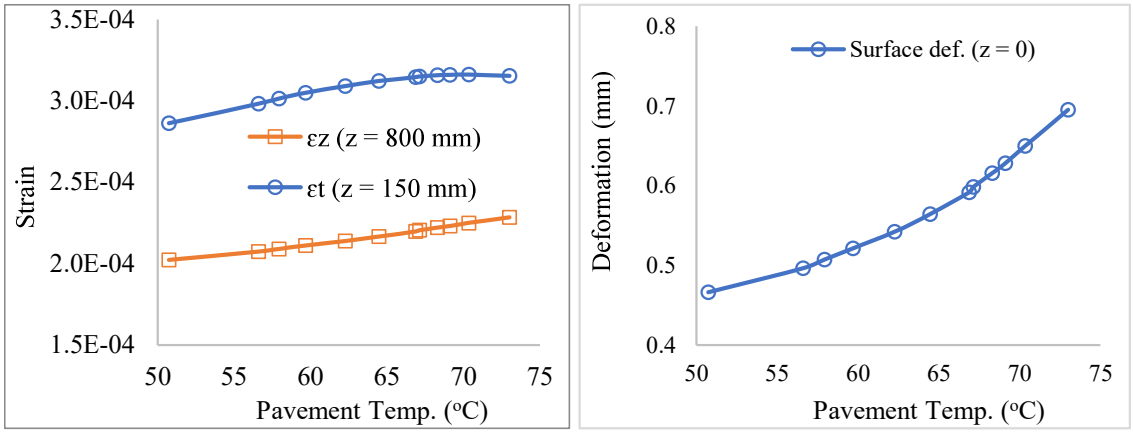

(a) (b)

Figure 6.7. Effect of extreme temperature on (a) ε_z and ε_t and (b) surface deformation.

As shown in Figure 6.7 (a), ε_z and ε_t were not found much sensitive to changes in maximum pavement temperature. Compressive strain (ε_z) at the top of the subgrade was found to increase only by 12.98% with a change in maximum pavement temperature of 50.74 °C (Srinagar) to 73 °C (Phalodi). Horizontal tensile strain (ε_t) at the bottom of AC layer was found to increase by 10.17% for the same change in temperature. For the same increase in the temperature, N_R was found to decrease by 42.50%, whereas, N_f was found to increase by 87.51%. One of the reasons for the trend is because of the significant increase in the vertical deformation of the AC layer (see Figure 6.7b). These outcomes indicate that both the fatigue life of the AC layer and subgrade rutting are significantly affected by temperature variation, hence, proper attention should be given at the design phase to improve their life.

6.3.3 Effect of layer thicknesses

In order to study the effect of layer thickness variation on the selected pavement structure, sensitivity analyses of layer thicknesses with respect to their structural responses as

shown in Figure 6.8 (a-b) were done using WMM as conventional base layer. The subgrade rutting (N_R) and fatigue life of the AC layer (N_f) were also estimated (see Figure 6.8 c-d). In the FE model, AC layer thickness was varied in the range of 100 mm to 200 mm, whereas, base layer and subbase layer thickness were varied between 150 mm to 310 mm. These ranges were selected as per the minimum specified limits [20].

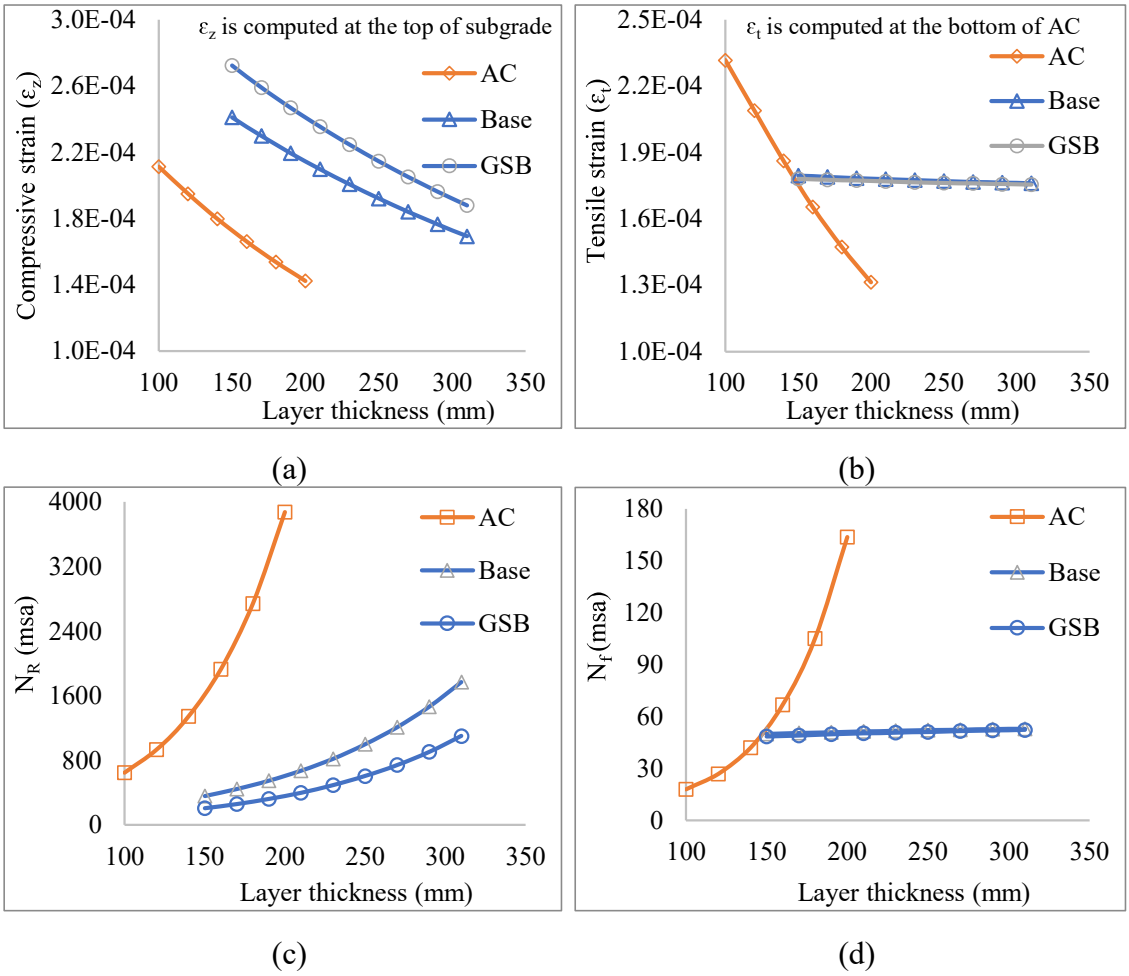

Figure 6.8. Effect of layer thickness on (a) ε_z, (b) ε_t, (c) N_R, and (d) N_f.

As shown in Figure 6.8(a), a reduction of 32.64% in ε_z was found when AC thickness increased from 100 mm to 200 mm, whereas, a reduction of 22.17% and 23.25% was found when base and subbase layer thickness was increased in the same range respectively. Although an increase of thickness by 100 mm in the AC layer, reduces ε_t by 43.33% as shown in Figure 6.8(b), however, with the same increase in thickness in the base and subbase layers, the values reduce by only 1.07% and 1.40% respectively. It can

be concluded that, increase in any layer thickness above subgrade significantly reduces ε_z at the top of the subgrade. However, if ε_t is required to limit, only asphalt layer thickness shall be increased.

On the basis of the obtained values of ε_z and ε_t, pavement life against rutting and fatigue was evaluated as shown in Figure 6.8(c-d). It was found that, subgrade rutting life (N_R) improves by about 500% (see Figure 6.8c) with an increase of 100 mm of AC thickness from 100 mm to 200 mm, whereas, an improvement of 179% and 194% was observed with the similar changes in base and subbase layer thicknesses. Similar plots for fatigue life (N_f) as shown in Figure 6.8(d), show that increase in AC layer thickness significantly improves its fatigue life performance. It was found that an increase in AC thickness by 100 mm (from 100 mm to 200 mm), increase its fatigue life by about 811%. However, increase in base and subbase layer thickness has no significant effect on the fatigue life of asphalt layer, which is expected. A similar increase in base and subbase thicknesses only manages to improve fatigue life of asphalt layer by 4.26% and 5.60% respectively.

6.3.4 Effect of emulsion treated stabilized base

Emulsion-treated aggregate (ETA) base layer is one of the popular choices to form a more stabilized base layer, in which aggregates are treated with slow-setting bitumen emulsion. Apart from increasing the base layer strength, ETA allows for the use of reclaimed asphalt pavement material. Even with the above benefits, as reported in different research studies, ETA has not been widely used in many countries like India primarily because of the lack of understanding and design guidelines. Since ETA increases the base layer strength, it in turn makes the overall pavement structure stronger. The increase in strength can be used in different ways, for example, to reduce the top layer thickness which will, in the

end, decrease the use of natural resources; or to compensate for overloaded layers which will prevent the possible reduction of the design life.

It is apparent that the inclusion of the ETA layer will strengthen the whole pavement structure, however, the exact benefit in percentage is yet unknown, particularly in other higher layers. The FE model proposed in an earlier chapter (see chapter 3), was used to have a deeper insight. At first, considering the same cross-section of pavement with the same loading, the percentage enhancement in the performance was studied considering a layer with WMM (material properties as shown in Table 6.1) as a reference. After that, parametric analyses were carried out in which the AC layer thickness was reduced in sequence for both the reference structure (with WMM) and the structure with the ETA layer (material properties as shown in Table 4.2). The effect of ETA on maximum surface deformation (z = 0) and strain (ε_t and ε_z) were analysed as shown in Figure 6.9(a -b) for comparison with a conventional base layer. The percentage change in critical strains ε_t and ε_z were evaluated for both the pavement structures (WMM and ETA) as shown in Figure 6.9(c -d). These strain values were further used to estimate AC fatigue and subgrade rutting life as shown in Table 6.5. On the basis of the output of the analyses, a table (see Table 6.5) was presented which summarizes different combinations of thickness and the response of structure.

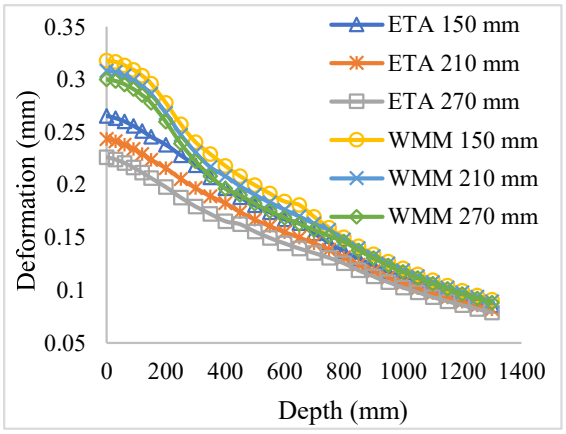

(a)

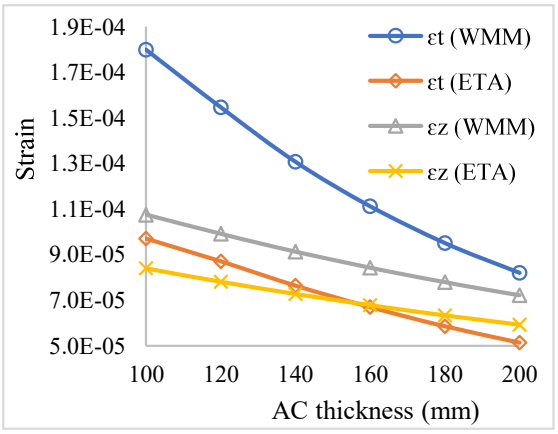

(b)

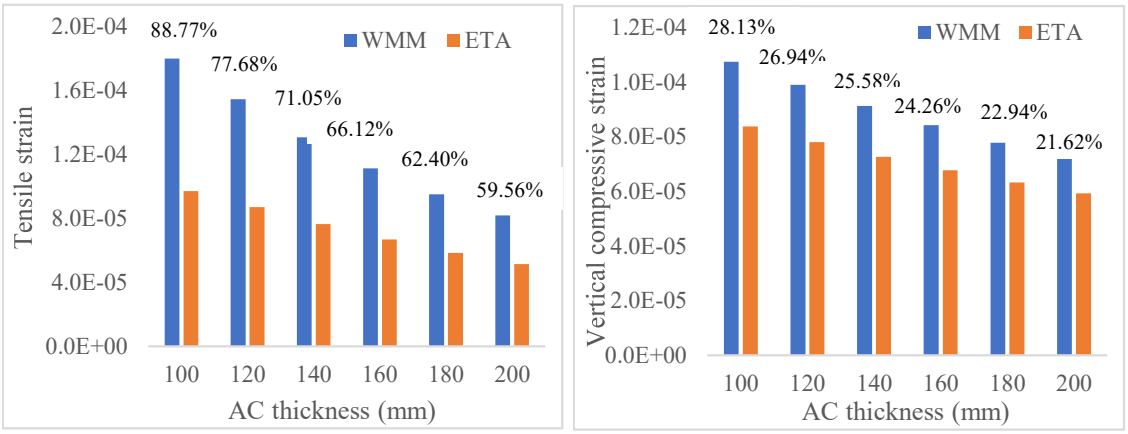

(c) (d)

Figure 6.9. Effect of ETA on (a) maximum deformation, (b) strains (ε_t at bottom of AC and ε_z at top of the subgrade layer), (c) % change in ε_t, and (d) % change in ε_z.

As shown in Figure 6.9 (a), it was found that the use of ETA results in a significant reduction in maximum deformation in the AC layer. For example, AC deformation in the case of 150 mm ETA base was found to reduce by 19.84% as compared to the same thickness of the conventional base. This reduction in AC deformation further increases with the increase in ETA thickness. The critical strains, ε_t and ε_z as shown in Figure 6.9 (b) were found to decrease with an increase in AC layer thickness for both conventional and ETA base pavement.

Table 6.5. Effect of ETA on subgrade rutting and AC fatigue life

AC layer thickness (mm)	N_R (msa)		N_f (msa)	
	WMM	ETA	WMM	ETA
100	695	2369	18	407
120	1015	3241	28	435
140	1482	4479	46	539
160	2146	5956	74	720
180	3096	8164	119	996
200	4407	11274	188	1395

The comparative changes in strain values for two different base layers were evaluated as shown in Figure 6.9 (c-d). It was observed that for a thinner AC layer (100 mm), the percentage change in ε_t (88.77%) and ε_z (28.13%) is more compared to thicker AC (200 mm) 59.56% and 21.62% respectively. Thus, it can be concluded that the effect of ETA stabilization is more prominent for lower AC thickness. From the above analysis, it can also be seen that the effect of ETA on ε_t is much higher (maximum of 88.77%) than as compared to ε_z (maximum of 28.13%).

Parametric analysis with varying thicknesses of the AC layer was done. As shown in Table 6.5, for the same thickness of the conventional base as that of ETA (300 mm), the rutting life of the subgrade with ETA was found to improve by 155.82 to 240.86% when AC thickness varies from 200 to 100 mm. For similar conditions, the fatigue life of the AC layer was found to improve by 642.02 to 2161.11%. It can be concluded that, ETA has a higher impact on the fatigue life of the AC layer as compared to the rutting life of the subgrade and it improves fatigue performance of the pavement manifold as compared to rutting performance.

The benefits of ETA in improving rutting and fatigue life of asphalt pavement were further used to explore the possibility of reduction in asphalt layer thickness. Considering a fixed layer thickness of conventional base and asphalt layer, ε_t and ε_z were evaluated. Taking this value of ε_t and ε_z as reference, new layer thickness of asphalt layer was evaluated in case of ETA used as stabilized base layer. Table 6.6 shows the possible reduction in asphalt layer thickness with the use of ETA as stabilized base.

Table 6.6. Performance of stabilized base (ETA) with varying AC thickness

AC thickness with WMM	AC thickness with ETA	ε_t (microstrains)		ε_z (microstrains)		Reduction in AC thickness
		WMM	ETA	WMM	ETA	
160 mm	100 mm	156.40	101.10	162.20	158.70	60 mm
180 mm	120 mm	138.60	99.34	149.60	148.10	60 mm
200 mm	140 mm	123.30	94.04	138.40	137.90	60 mm
215 mm	160 mm	113.00	87.29	130.70	129.50	55 mm
230 mm	180 mm	103.70	80.31	123.50	120.80	50 mm
250 mm	200 mm	92.79	73.65	114.30	112.50	50 mm

As shown in Table 6.6, it was found that if ETA is used as the stabilized layer, it may help in the reduction of the top layer thickness without compromising the performance of the whole structure. For example, by limiting ε_z value to 158 microstrains for both cases (with ETA and without ETA) the required thickness of the AC layer is reduced by 60 mm (from 160 mm to 100 mm). Parametric analyses of possible thickness reductions in the AC layer for different conditions (ε_z and ε_t) are given in Table 6.6 which can help pavement designers for adequate design thickness choices. The results are obtained only considering these two criteria and a standard set of input conditions for an ideal pavement section (see Section 3.4.1), Hence, further investigation should be done before using them in practice.

As discussed above, ETA has significant potential to improve rutting and fatigue life of asphalt pavement. However, it is important to study the effect of ETA on the stabilized base layer itself as compared to conventional base. Since, addition of bitumen emulsion and cement increases stiffness of the material and may result in higher horizontal tensile strain at the bottom of ETA base layer. To study the effect of stabilization on ETA layer

itself as compared to conventional base, load was varied from 40 to 80 kN and ε_t and ε_z at the bottom of base layer was noted as shown in Figure 6.10.

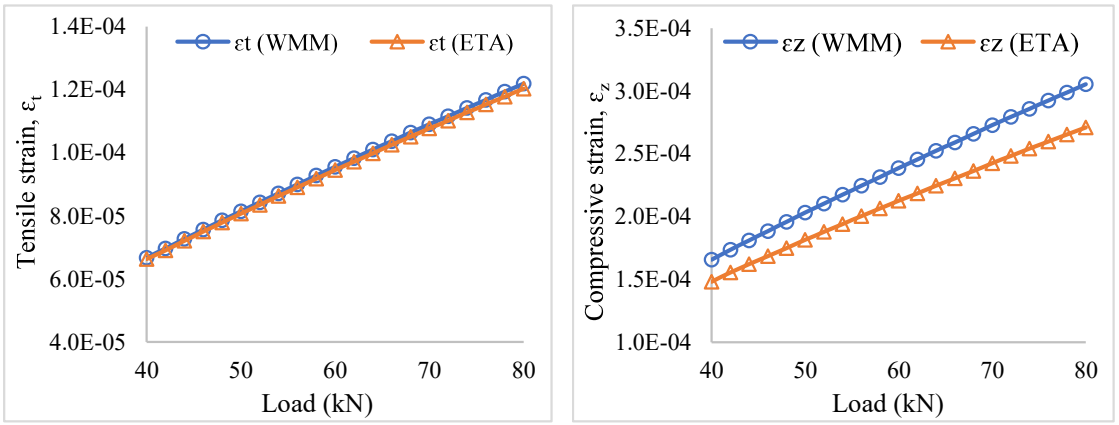

(a) (b)

Figure 6.10. Effect of stabilization on the base layer response (a) ε_t (z = 450 mm) and (b) ε_z (z = 450 mm).

It was observed that, emulsion treated stabilized base reduces ε_t significantly in asphalt layer (see Figure 6.9 (b)), however, there is almost no change in ε_t value in stabilized base layer as compared to conventional base subjected to different loading conditions (see Figure 6.10 (a)). So, it can be concluded that, fatigue life of emulsion treated base is similar to conventional base. ETA was found more effective in improving rutting life of the base layer, as ε_z at the bottom of stabilized base layer was found lesser (average reduction is 21.44%) than in case of conventional base.

6.3.5 Performance of emulsion treated base in overloading cases

Overloading is a major concern in many of the developing nations including India and causes significant damage to AC pavement. It was found that an AC pavement which is generally designed for 15 years when subjected to 5% of overloading, the design life is reduced by 2.7 years [267]. Due consideration in the design phase itself is needed to take care of overloading-related pavement damage. Structural safety of the pavement against overloading can be ensured by increasing the layer thicknesses or improving the stiffness

of existing layers. The focus of the previous section was to evaluate the potential reduction in the thickness of the AC layer with the use of the ETA layer, this section considers the scenario where instead of changing the AC layer thickness, various overloading situation is analysed. The critical parameters considered in pavement analysis (ε_t and ε_z) were evaluated for both conventional base and stabilized base layer under increasing overloading situations as shown in Figure 6.11.

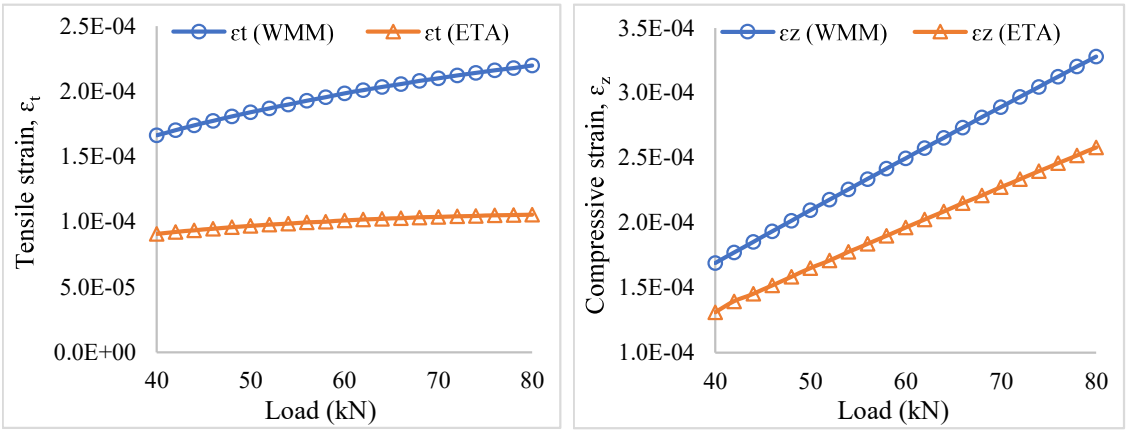

(a) (b)

Figure 6.11. Effect of base layer stabilization on the pavement responses (a) ε_t (z = 150 mm) and (b) ε_z (z = 800 mm) in overloading cases.

As shown in Figure 6.11, it was found that, base layer stabilization with emulsion treatment results in better performance in asphalt layer fatigue as compared to subgrade rutting life. It significantly reduces horizontal tensile strain (average reduction was found to be 48.93%) at the bottom of asphalt layer. The vertical compressive strain at the bottom of the subgrade layer was found to reduce by 21.44% under similar overloading conditions. It can be concluded that, ETA provides better resistance to fatigue cracking in asphalt layer in overloading conditions and it can be used to replace conventional bases where frequent overloading related fatigue failure of the asphalt pavement is observed.

The very next question arises, how much overloading can be taken care by ETA when used as stabilized base layer. To study the benefits of stabilization in terms of overloading

leverage, the vertical load was increased keeping all other parameters (ε_t and ε_z) the same as given in Table 6.7. This study will provide a choice of selection of materials in base layers based on loading conditions.

Table 6.7. Effect of ETA on pavement performance and overloading leverage

Base	**Thickness (mm)**	**Load (kN)**	**ε_z (microstrains) at z = 800 mm**	**N_R (msa)**	**ε_t (microstrains) at z = 150 mm**	**N_f (msa)**
WMM	300	40	168.90	1787	166.30	60
ETA	300	51	167.70	1845	97.39	483
WMM	250	40	187.50	1113	167.00	59
ETA	250	50	187.20	1121	99.32	447
WMM	200	40	209.10	679	167.80	58
ETA	200	48	206.20	723	102.10	402
WMM	150	40	234.40	404	168.90	57
ETA	150	47	234.20	406	107.90	324

To have an easier interpretation of the results, keeping 40 kN with the WMM layer as a reference case, the simulations were repeated with ETA pavement structure until equivalent load resulting in similar strains were found, as shown in Table 6.7. In terms of benefits, pavements built with an ETA base provided 11 kN to 7 kN (27.5 to 17.5%) leverage depending on the thickness of the ETA considered. Corresponding benefits in N_R and N_f values for different loading combinations are also presented in the same table.

6.4 Pavement response using LVE AC and linear elastic UGMs

This section of study considers linear viscoelastic properties of asphalt mixes (BC-2) as discussed in Chapter 4 and linear elastic properties of unbound granular layers based on CBR test results as shown in Table 6.1. Same FE model of test tire has been used to

simulate realistic nonuniform contact stress distribution at tire-pavement interface as done in previous stage of simulation. This analysis will help in understanding the effect of linear viscoelastic properties of asphalt mixes on the structural response of asphalt pavement especially on the fatigue life. With the use of linear elastic properties of these mixes in current practice, whether we are underestimating or overestimating the material strength can also be highlighted. The parametric analysis considering effect of loading, air voids in the mixes, temperature, and layer thickness on the structural response of asphalt pavement and its life in rutting and fatigue has been presented in this section. Results of the analysis will be further compared with linear elastic properties in the previous simulation.

6.4.1 Effect of loading

The details of loading, its importance, legal limit, and concern of overloading for asphalt pavement analysis and design has already been discussed in previous section. It was shown that how significantly overloading reduces pavement life in rutting and fatigue if linear elastic properties of various materials in pavement layers are considered.

Since, linear viscoelastic properties of asphalt mix (BC-2) have been considered in present simulation, the main idea of the analysis was to find if consideration of viscoelastic properties of these mixes affect pavement life in case of overloading. The standard single axle load of 80 kN (40 kN on one tire) was considered as reference load and overloading of 25% to 100% was considered in the analysis. These results will be later compared with the outcomes of linear elastic case. The analysis will help in understanding importance of material characterization of asphalt mixes.

The maximum deformation in the pavement and normal strain just below the tire load has been plotted against pavement depth as shown in Figure 6.12. The vertical compressive

strain (ε_z) and stress (σ_z) at the top of the subgrade layer (z=800 mm) as well as horizontal tensile strain (ε_t) and stress (σ_t) at the bottom of the asphalt layer (z=150 mm) has been plotted against loading as shown in Figure 6.12 to see the effect of overloading on these critical points.

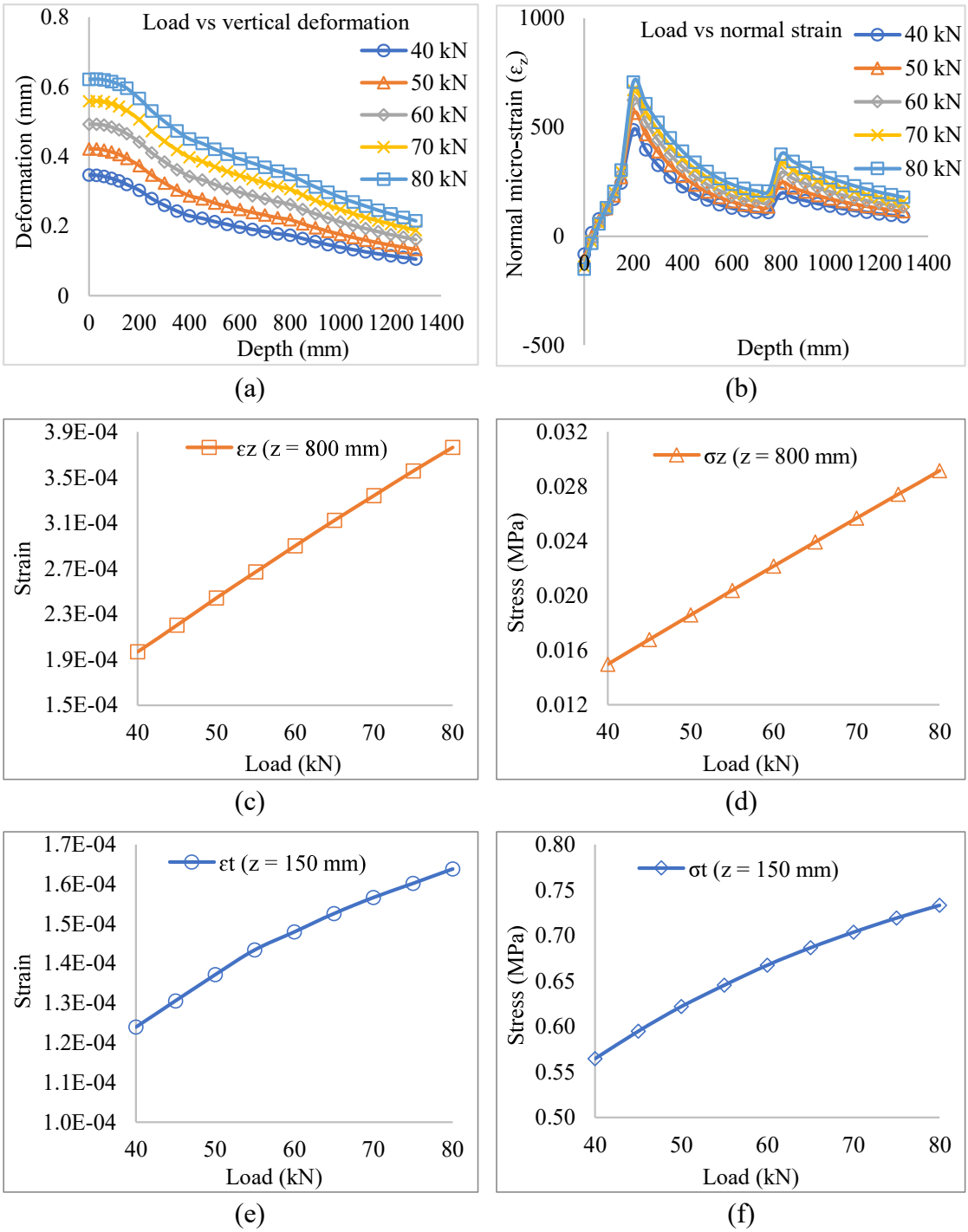

Figure 6.12. Effect of loading on LVE response of the pavement.

Considering the LVE properties of asphalt mixes, it was found that, maximum surface deformation and normal strain in various layers is higher as compared to linear elastic considerations. The variation of the obtained pavement response was found similar as in case of linear elastic analysis. As shown in Figure 6.12, effect of loading on ε_z and σ_z is also higher for LVE simulation. With increase in loading, the percentage increase in ε_t and σ_t were found similar to that in case of linear elastic analysis. However, LVE simulation results in lesser ε_t and σ_t. It can be concluded that, in case of static analysis, LVE simulation yields higher fatigue life while lower rutting life of the asphalt pavement. To make ease of understanding, the data of Figure 6.12 is presented in tabular form with their respective percentage changes in Table 6.8 and effect of overloading on rutting life of the asphalt pavement is shown in Figure 6.13.

Table 6.8. Effect of loading on the pavement response using LVE simulations

Load	**40 kN**	**50 kN**	**60 kN**	**70 kN**	**80 kN**
Overloading (%)		25	50	75	100
Maximum deformation	0.347	0.422	0.492	0.559	0.621
% increase in deformation		21.610	41.780	61.090	78.960
ε_z (micro-strains) at top of the	196.960	244.281	289.979	334.014	376.363
% increase in ε_z		24.025	47.291	69.584	91.086
ε_t (micro-strains) at the bottom of	123.993	137.190	148.002	156.505	163.882
% increase in ε_t		10.643	19.363	26.221	32.170
Subgrade rutting life, msa (N_R)	890	335	154	81	47
% reduction in rutting life		62.330	82.696	90.880	94.690

It should be noted that, effect of overloading on the pavement response considering LVE properties of asphalt mixes are similar to that of linear elastic considerations. The change in critical mechanistic parameters (ε_t and ε_z) as shown in Table 6.8 were found close to the stage 1 simulations (linear elastic). However, this is important to note that,

consideration of LVE properties of asphalt mixes predicts higher maximum surface deformation, average deformation in various layers, and normal compressive strain (ε_z) in the pavement while it predicts lower value of horizontal tensile strain (ε_t) as compared to linear elastic properties of asphalt mixes.

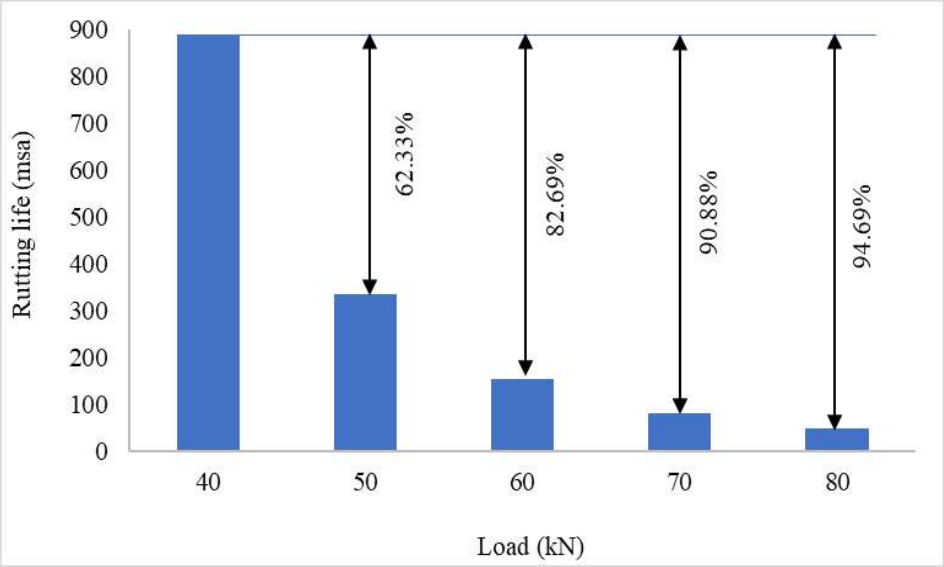

Figure 6.13. Effect of loading on rutting life using LVE simulations.

As shown in Table 6.8, rate of increase of maximum surface deformation with respect to overloading is constant and it was found to increase at a rate of nearly 19.74% per 25% of increase in loading. Similar trends were obtained for ε_z and it was found to increase at an average rate of 22.77% per 25% of increase in loading. However, the effect of loading on ε_t was not found that significant as in earlier cases. The rate of increase of ε_t was found to be 8.04% for every 25% increase in loading. The empirical relations used to evaluate fatigue life of the asphalt pavement as per the guidelines of IRC:37 is based on ε_t and M_r of asphalt mixes. Since M_r of mixes are based on linear elastic properties so it is difficult to directly corelate these modulus values with LVE properties of the mixes. Therefore, fatigue life of the pavement has not been shown in Table 6.8. However, rutting life of the asphalt pavement (N_R) is based on ε_z value only. So, it was evaluated for current LVE simulations as shown in Table 6.8 and Figure 6.13. It is important to note that, although,

the average rate of increase of ε_z is 22.77% only with every 25% increase in loading, the rutting life of the pavement deteriorates at much faster rate. For an overloading of 25% (from 40 kN to 50 kN), N_R reduces by 62.33%. However, this rate of decrease of N_R keeps on reducing and it was found that for further increase of 25% loading, the N_R value reduces by 20.36% only.

6.4.2 Effect of air void in the asphalt mix

The effort in pavement compaction is important as it decides the final performance. Air voids are generally described as the most effective parameter to explain the behaviour of asphalt mix. Compaction imparts durability and resistance to deformation by locking bitumen coated aggregate particles together. So, it has significant effect on strength and durability of the asphalt mixture.

In this stage of simulation, the FE model of asphalt pavement system uses the linear viscoelastic properties of asphalt mixes and linear elastic properties of unbound granular layers as discussed earlier. It is well known that, the compactive effort has huge role in controlling air void in the asphalt mix. During pavement construction, sometimes lack of proper quality control in compaction activity (temperature of asphalt mix is not maintained during laying, lower or higher compactive effort than design) results in different air voids than specified. So, it is important to understand the role of air voids on the structural response of asphalt pavement. The critical pavement response parameters (ε_z and ε_t) ultimately define pavement life in rutting and fatigue. So, it is crucial to evaluate these mechanistic parameters in this study. The plot of vertical deformation and normal compressive stress, σ_z (z-z) against pavement depth at 4, 5, and 6% air void has been presented in Figure 6.14. σ_z has been plotted at log scale as the stress gradient is steep and reduces significantly in a small vertical depth domain. The ε_z and ε_t has also

been evaluated to estimate pavement life in rutting and fatigue as shown in Figure 6.15. Initially, the ε_z has been determined at various nodal points throughout the pavement depth and later it has been specifically reported at z = 800 mm (top of the subgrade layer) to evaluate rutting life. However, the ε_t value has been evaluated at z = 150 mm (at the bottom of the asphalt layer) only corresponding to 4, 5, and 6% of air voids in the asphalt mix to evaluate fatigue life of the pavement.

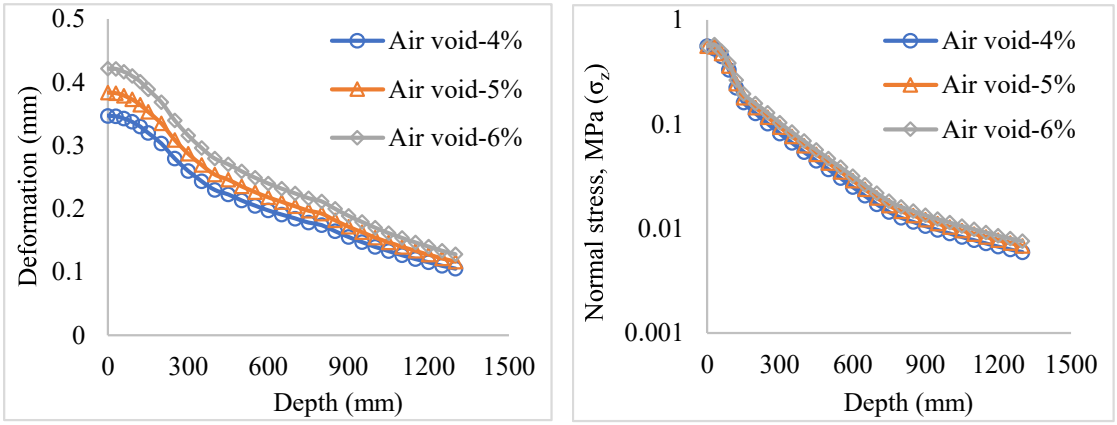

Figure 6.14. Effect of air void on deformation and σ_z under LVE simulations.

The rate at which σ_z subsides initially against pavement depth is steeper than deformation. The stress reduction of 71.10, 67.83, and 64.93% was observed at air voids of 4, 5, and 6% respectively in the BC-2 layer. This is because the top layer of BC-2 has the highest stiffness among all the layers and is much higher than its subsequent base layer. So, most of the stress is taken by the bituminous concrete layer. It was also interesting to note that at a higher air void in the mix, the percent reduction in stress in the BC-2 layer was lesser than at a lower air void. This is due to the higher stiffness of the mix at lower air void giving a more compact structure and thus stress dissipates more quickly within the layer. Whereas, the opposite trend prevails in the case of deformation. As the material stiffness of the upper layers is higher than lower layers, so, the rate of subsidence of deformation is much lesser in BC-2 layer. Only 7.84% of deformation were found to reduce corresponding to 4, 5, and 6% of air voids in this layer, and most of the surface

deformation was found to subside in the natural subgrade and compacted subgrade layers. The effect of air void on the structural response of the asphalt pavement was found significant. As shown in Figure 6.14, maximum surface deformation was found to increase by 10.52 and 21.58% respectively when air void in the asphalt mixture (BC-2) increases from 4 to 5% and 6% respectively. Similar results were obtained for σ_z also. An average increase of 13.34% and 24.26% in σ_z value was obtained for the same change in air void as in previous case. In addition to surface deformation and normal stress, the two critical mechanistic parameters (ε_z and ε_t) were also determined with the help of FE model to obtain rutting and fatigue life of the pavement as shown in Figure 6.15.

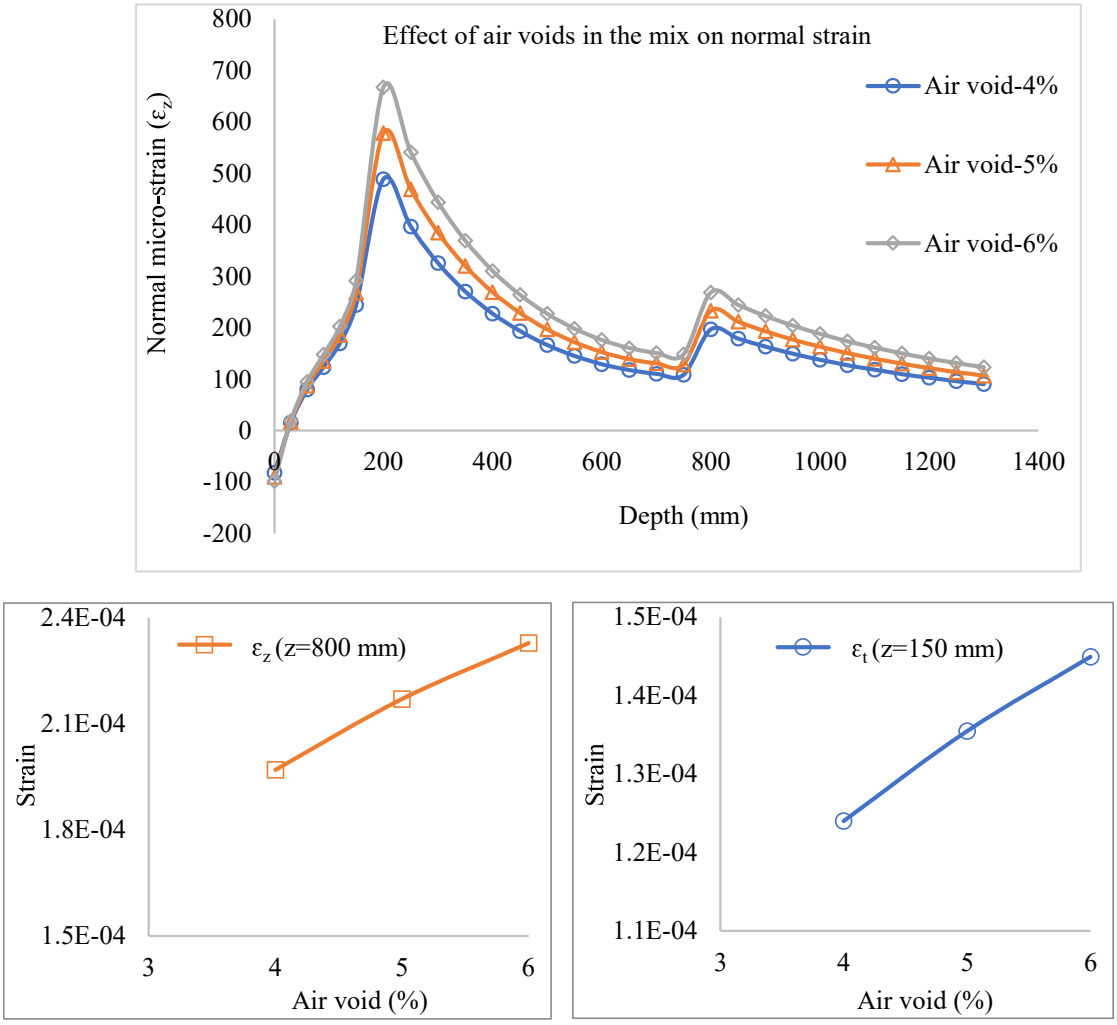

Figure 6.15. Effect of air void on ε_z and ε_t under LVE simulations.

As shown in Figure 6.15, the average increase in ε_z value was found to be 13.29% and 22.56% when air void in the asphalt mixture rises from 4 to 5% and 6% respectively. The rise in ε_z is higher in lower layers due to increased difference in layer stiffness. The ε_z value at z = 800 mm at an air void of 5% and 6% was found 10.15% and 18.20% higher than at 4% air voids. The effect of air void on horizontal tensile strain at bottom of the asphalt layer were also similar to the results of ε_z. For the same change in air voids, ε_t was found to increase by 9.26% and 16.88% respectively. Based on obtained ε_z at different air voids in the asphalt mixes, subgrade rutting life of the pavement (N_R) was evaluated as shown in Figure 6.16.

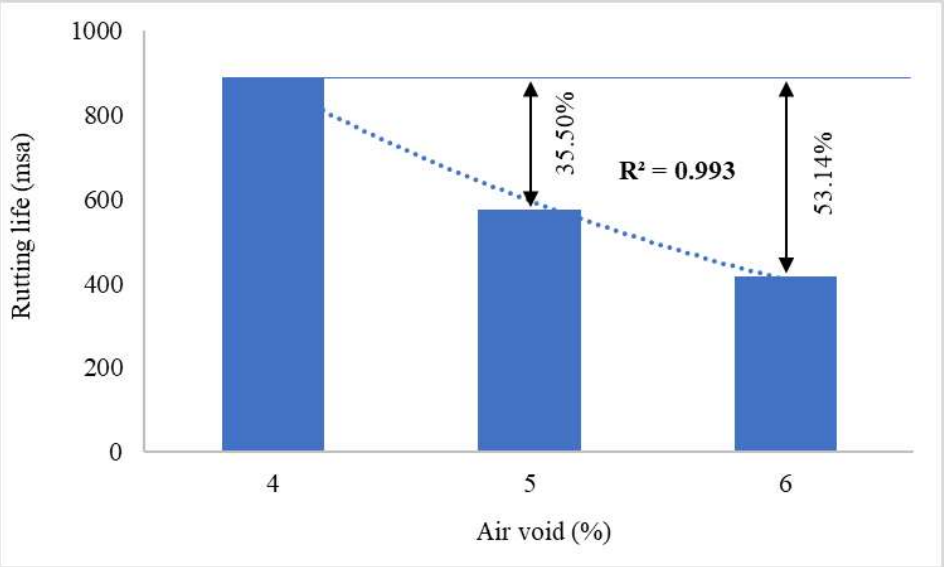

Figure 6.16. Effect of air void on rutting life considering LVE properties of AC.

As shown in Figure 6.16, the subgrade rutting life was found to decay exponentially with the increase in the air voids in the mix. Although, effect of air void on the structural response of asphalt pavement is not that significant as it seems in subgrade rutting life. It was found that, an increase of 1% of air void from 4 to 5%, reduces N_R by 35.50%. It is a significant effect on pavement performance considering subgrade rutting life. It suggests the importance of quality compaction in field to meet desired pavement performance.

6.4.3 Effect of temperature on LVE response of asphalt pavement

The temperature of asphalt mix is considered as one of the major environmental factors which affects pavement performance severely. The damage to asphalt pavement due to rise in temperature draws attention of pavement engineers to look how it affects damage rate (deformation, stress, and strain distribution in pavement layers) in asphalt pavement and how it can finally affect pavement life. Since, asphalt layer is considered as viscoelastic, a change in temperature directly affects its modulus value. The subsequent change in asphalt layer modulus modifies the stress distribution in the pavement layers which may lead to loss of pavement life. So, based on local temperature, suitable grade of binder is selected for the preparation of asphalt mix. The viscoelastic nature of asphalt makes it temperature sensitive and thus has an obvious effect on asphalt rutting, subgrade rutting, and fatigue life. Asphalt layers are prone to thermal and fatigue cracking at low temperature as it becomes hard and brittle. However, at higher temperature, it becomes soft and thus it is more prone to rutting. Since, properties of asphalt mixes changes with temperature variation; therefore, its response to axle loading will also be different. The increase in temperature reduces material stiffness and load bearing capacity of asphalt mix and thus higher fraction of load induced stress is transmitted to lower layers which ultimately affects the material response in base, subbase, and subgrade layer.

Thus, effect of temperature on the structural response of asphalt pavement, its damage, and performance cannot be ignored and need full scale study. The range of temperature has been selected based on seasonal variation and extreme temperature conditions during winter and summer. Although, the highest temperature during summer is below 55^{o} C, the analysis has been extended to 70^{o} C to include maximum surface temperature as discussed in stage II simulation. Creep compliance test has been conducted on asphalt

mixes (BC-2) at 5, 15, and 25° C to evaluate its viscoelastic properties. However, looking into the temperature variation over the year in India and maximum surface temperature, creep compliance data with time was also evaluated for a temperature of 40, 55, and 70° C using Williams-Landel-Ferry (WLF) equation [200]. The WLF equation (see Eq. 6.7) allows for the estimation of material properties beyond test data using time temperature superposition principle (TTSP). The application of TTSP for materials exhibiting nonlinear behaviour, experiencing large changes in physical structure due to temperature variations, aging process may lead to inaccurate results. The shift factor may not accurately capture the complex changes in material properties under significant structural changes at higher temperatures. The TTSP assumes uniform behaviour of material, which may not hold true for heterogeneous materials. Also, applying TTSP to complex stress states, like multiaxial loading, can be challenging due to nonlinear interaction between different stress components. Keeping these limitations in mind, mixes should be stressed to a limit, which produces strain within the LVE regime. Also, test should not be carried out at higher temperatures, where asphalt mixes experience large strains beyond LVE response.

$$\log(a_T) = -C_1 \times \frac{T - T_R}{C_2 + (T - T_R)} \tag{6.7}$$

where, a_T is the WLF shift factor, T is the temperature, T_R is the reference temperature selected to construct the creep compliance master curve, and C_1 and C_2 are model constants adjusted to fit the values of the superposition parameter a_T. This equation can be used to fit discrete values of the shift factor, a_T vs temperature. The evaluated shift factor and WLF model constants are shown in Table 6.9.

Table 6.9. Shift factor and WLF constants for various temperatures

Temperature (°C)	**5**	**15**	**25**	**40**	**55**	**70**
a_T	3.982	1.923	1.000	0.420	0.198	0.102
WLF constants	C_1 – 5.330 and C_2 – 197.635					

These shift factors were further used to determine creep compliance data at unknown temperatures of 40, 55, and 70° C as shown in Figure 6.17. The experimentally determined creep compliance data at temperatures of 5, 15, and 25° C has already been presented in chapter 4.

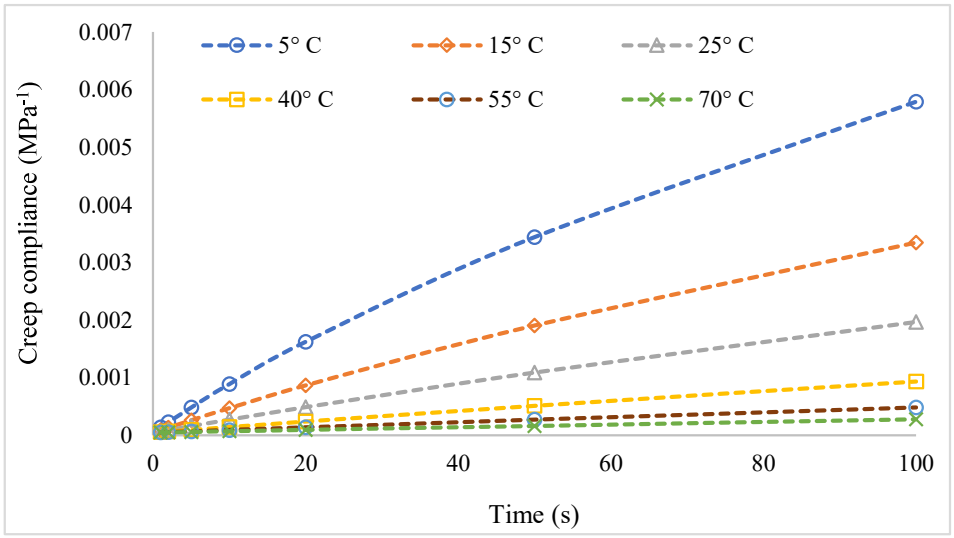

Figure 6.17. Time-temperature dependency of creep compliance.

These creep compliance data were further used to evaluate Prony series constants as discussed in Chapter 4 to be used as an input parameter in FE model of asphalt pavement system. The structural response (vertical deformation, normal strain, and horizontal tensile strain) was evaluated using FE model of asphalt pavement system (considering realistic solid tire body) at different test temperatures as discussed earlier. The variation in these structural parameters were obtained with the change in temperature and performance in subgrade rutting and asphalt concrete fatigue was determined. The effect

of mix temperature on the structural response (deformation and normal strain) of the asphalt pavement is shown in Figure 6.18.

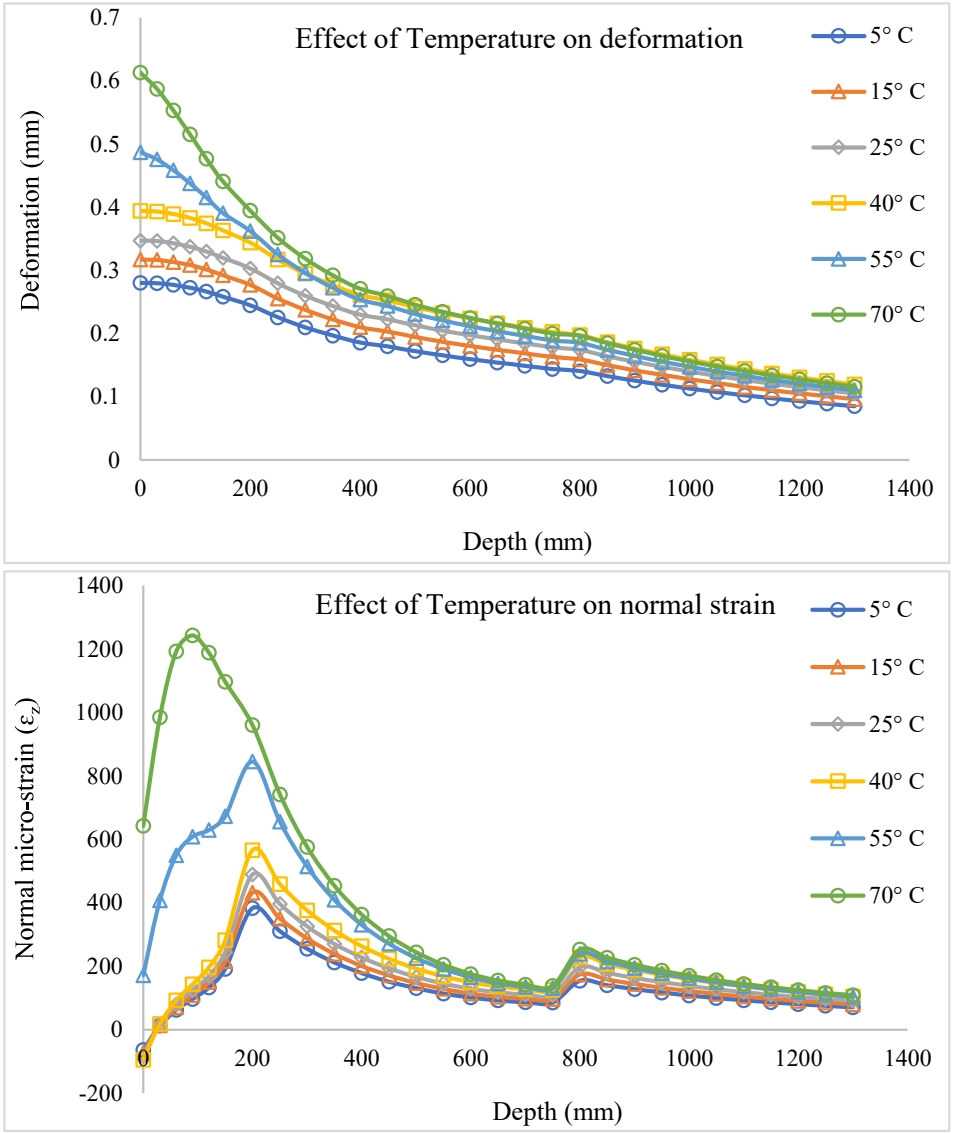

Figure 6.18. Effect of temperature on vertical deformation and ε_z under LVE simulations.

The effect of temperature on pavement deformation and normal strain is significant as shown in Figure 6.18 and it need to be discussed numerically in terms of percentage change to have an exact idea of temperature influence. The maximum surface deformation was found to increase by 13.11, 23.82, and 40.55, 73.72, and 118.64% when temperature rises from 5° C to 15, 25, 40, 55, and 70° C respectively. At lower temperatures, asphalt mix are stiff and resistance to deformation due to loading is higher. However, as

temperature increases, asphalt mix softens due to viscoelastic behaviour of binder and allows higher penetration into it which leads to higher deformation. It is important to note that, the rate of change in maximum surface deformation at higher temperature is also high. This is due to the higher loss in asphalt modulus at high temperatures. The reason of higher deformation in lower layers with rise in temperature is due to higher fraction of load induced stress shared by them. Since, at higher temperatures, modulus of asphalt layer reduces significantly; thus, the resistance to induced stress is also lower and hence higher fraction of stress is transmitted to lower layers.

Similar trends were obtained for normal strain also. The maximum normal strain was found to increase by 12.78, 27.74, 47.68, 120.69, and 224.55% respectively when temperature rises from 5° C to 15, 25, 40, 55, and 70° C respectively. It can be concluded that, temperature plays an important role in deciding the type of binder in asphalt mixture and in regions of higher ambient temperature, these mixes shall be characterized based on viscoelastic properties. The LVE characterization of the mixes can more realistically take care of the effect of temperature on mix behaviour. The critical mechanistic parameters ε_z (z = 800 mm) and ε_t (z = 150 mm) were also evaluated as shown in Figure 6.19 to see the effect of temperature on pavement performance in subgrade rutting and asphalt fatigue.

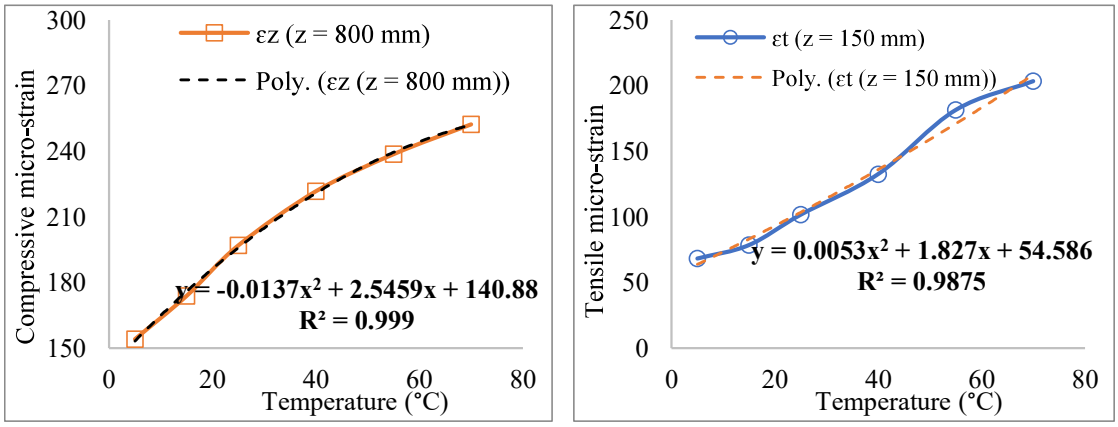

Figure 6.19. Effect of temperature on ε_z and ε_t under LVE simulations.

As shown in Figure 6.19, ε_z and ε_t follows quadratic variation with temperature. Initially, the slope of ε_t-temperature graph is positive; however, it seems to become negative at higher temperatures beyond 50° C. It means, the tensile strain in the asphalt layer will starts decreasing with further rise in temperature beyond zero slope line. This is important to note that, at higher temperatures near binder's softening point, the resistance to deformation in the mix offered by binder is almost negligible and the mix is viscous and soft which do not allow to develop significant tensile stress in the mix.

The ε_z (z = 800 mm) was found to increase by 12.78, 27.75, and 43.79, 54.87, and 63.65% when temperature rises from 5° C to 15, 25, 40, 55, and 70° C respectively. These variations in ε_z value are slightly higher than average normal strain variations. Since, normal strain includes tensile strain (negative) component also it reduces overall average ε_z value. The effect of temperature on ε_t (z = 150 mm) was found higher than ε_z (z = 800 mm). The ε_t was found to increase by 15.10, 49.06, 94.35, 166.05, and 198.13% with the increase in temperature from 5° C to 15, 25, 40, 55, and 70° C respectively. The slope of ε_t-temperature graph is not uniform and keeps on increasing with increase in temperature which leads to increasing rate of percentage increase in ε_t value.

These critical mechanistic strain parameter ε_z and ε_t were further used to estimate subgrade rutting and asphalt fatigue life to see the ultimate effect of temperature on pavement performance. Since, this stage of simulation considers LVE properties of asphalt mixes using creep compliance test, so linear elastic properties (resilient modulus of asphalt mix) is not available. However, fatigue performance equation as per the guidelines of IRC:37 uses resilient modulus of asphalt mix and tensile strain at the bottom of asphalt layer as an input parameter. The elastic modulus (M_R) of asphalt mix can be determined as a function of pavement temperature as per following equation [270]:

$$E = 15000 - 7900 \times \log(T) \quad (6.8)$$

where, E is elastic modulus of asphalt layer (MPa) and T is the pavement temperature (°C). The elastic modulus was first determined at test temperature of 5, 15, 25, 40, 55, and 70° C using Eq. 6.8 as shown in Table 6.10 and asphalt fatigue life (see Figure 6.20) was determined using Eq. 6.5 as mentioned earlier. The subgrade rutting life was determined using Eq. 6.4 based on ε_z at z = 800 mm as shown in Figure 6.21.

Table 6.10. Temperature variation of elastic modulus of mixes and fatigue life

Temperature (°C)	**5**	**15**	**25**	**40**	**55**	**70**
E_{AC} (MPa)	9478.13	5708.88	3956.27	2343.72	1251.13	423.72
ε_t, z = 150 mm (micro-strain)	68.24	78.54	101.72	132.62	181.55	203.44
N_f (msa)	762	680	340	189	95	154

As shown in Table 6.10, the stiffness of asphalt layer (elastic modulus) reduces exponentially with the increase in temperature as rise in temperature softens binder present in it leading to reduced resistance to deformation. The ε_t varies with temperature at an increasing rate which results in rapid loss of asphalt fatigue life.

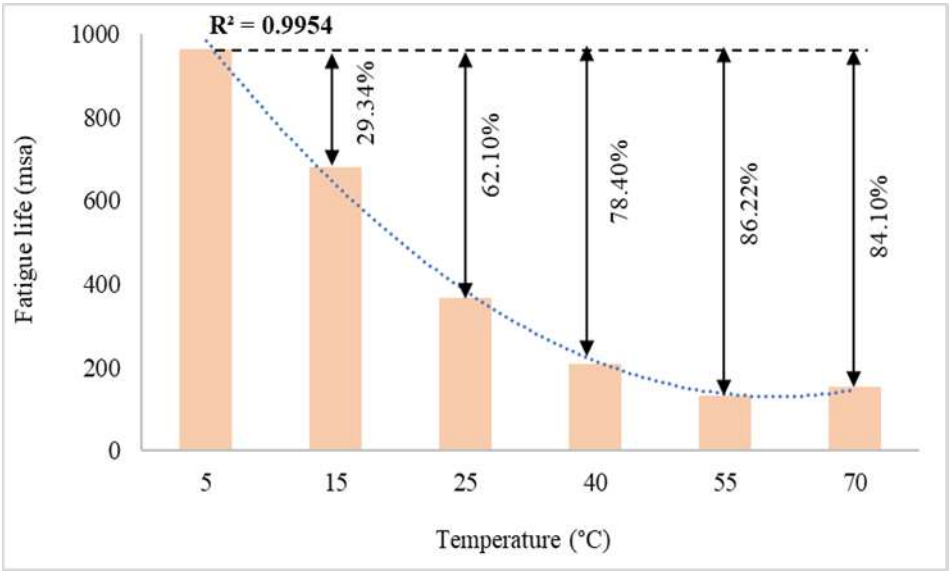

Figure 6.20. Effect of temperature on asphalt fatigue life.

The two input parameters (ε_t and M_R) used in the determination of asphalt fatigue life (see Eq. 6.5) is of opposing nature. The ε_t increases with increase in temperature at one end while the M_r value decreases sharply with same increase in temperature at another end. Since, the effect of temperature on ε_t is significant and it varies with higher power (see Eq. 6.5) than M_R, it becomes deciding factor in the variation of asphalt fatigue life. As shown in Table 6.10 and Figure 6.20, the fatigue life of asphalt layer was found to decrease by 29.34, 62.10, 78.40, 86.22, and 84.10% when temperature increases from 5° C to 15, 25, 40, 55, and 70° C respectively. It was found to vary exponentially. However, this variation changes at higher temperatures and fatigue life were found to increase at 70° C as compared to 55° C. This is due to the rate of change in ε_t reduces at higher temperatures as compared to lower temperatures.

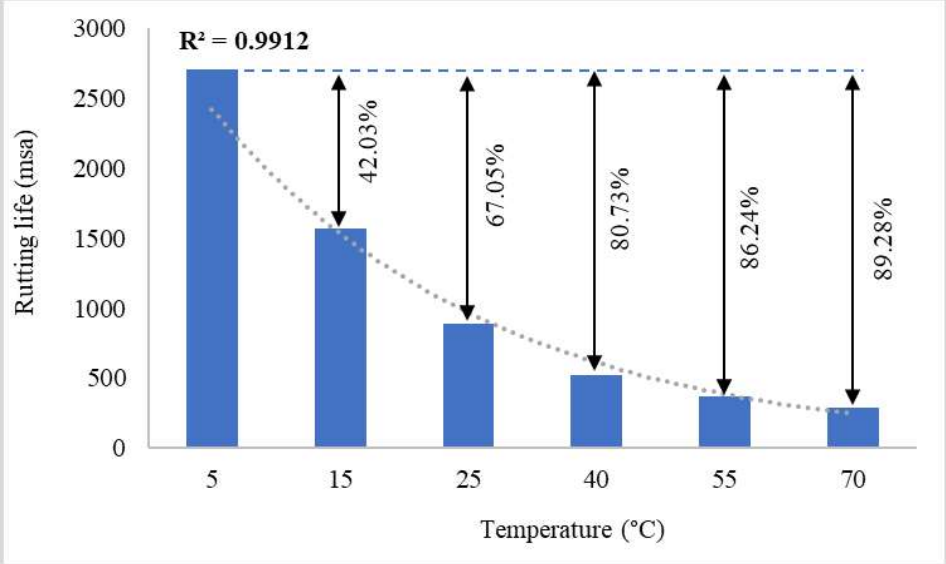

Figure 6.21. Effect of mix temperature on subgrade rutting life.

The effect of temperature on subgrade rutting life was found similar to that of asphalt fatigue life. As temperature increases, stiffness of top layer decreases which results in higher stress transfer to lower layers. This increases the compressive stress and strain in lower layers. The subgrade rutting varies as inverse power law of ε_z; thus, increase in ε_z reduces rutting life of the pavement. It was found that an increase in temperature from 5°

C to 15, 25, 40, 55, and 70° C, reduces subgrade rutting life by 42.03, 67.05, 80.73, 86.24, and 89.28% respectively. This analysis encourages to evaluate temperature dependent viscoelastic properties of asphalt mixes which can better estimate pavement performance in rutting and fatigue.

6.4.4 Effect of layer thickness on LVE response of asphalt pavement

The increasing stresses in asphalt pavement due to increased traffic loading results in pavement deformation in a short duration. The structural response of asphalt pavement is often controlled by increasing thickness of various layers mostly asphalt layer due to higher stiffness. This is considered as one of the key solutions to prevent pavement damage during design phase itself. The increase in top layer thickness, reduces ε_t and ε_z considerably which results in increased subgrade rutting and asphalt fatigue life. To understand this improvement in pavement life numerically, thickness of various layers was varied to see its effect on ε_t and ε_z and finally pavement performance.

The asphalt layer thickness in FE simulation was varied from 100 mm to 200 mm while base and subbase layer thickness was varied from 150 mm to 310 mm. It shall be noted that the thickness of asphalt layer is combined thickness of binder and surface course. The range of thickness variation in case of base and subbase layer is based on minimum thickness requirement as specified in IRC:37. The effect of asphalt layer thickness on the structural response of pavement (vertical deformation and normal) is shown in Figure 6.22. These responses have not been shown here against the variation in base and subbase layer thickness to avoid repetitions. However, the critical mechanistic parameters (ε_z and ε_t) have been evaluated to see the effect of variation of all the layers (asphalt, base, and subbase layer thickness) thickness. These parameters have been further used to estimate

the effect of these layer thicknesses on the pavement performance in terms of subgrade rutting and asphalt fatigue life.

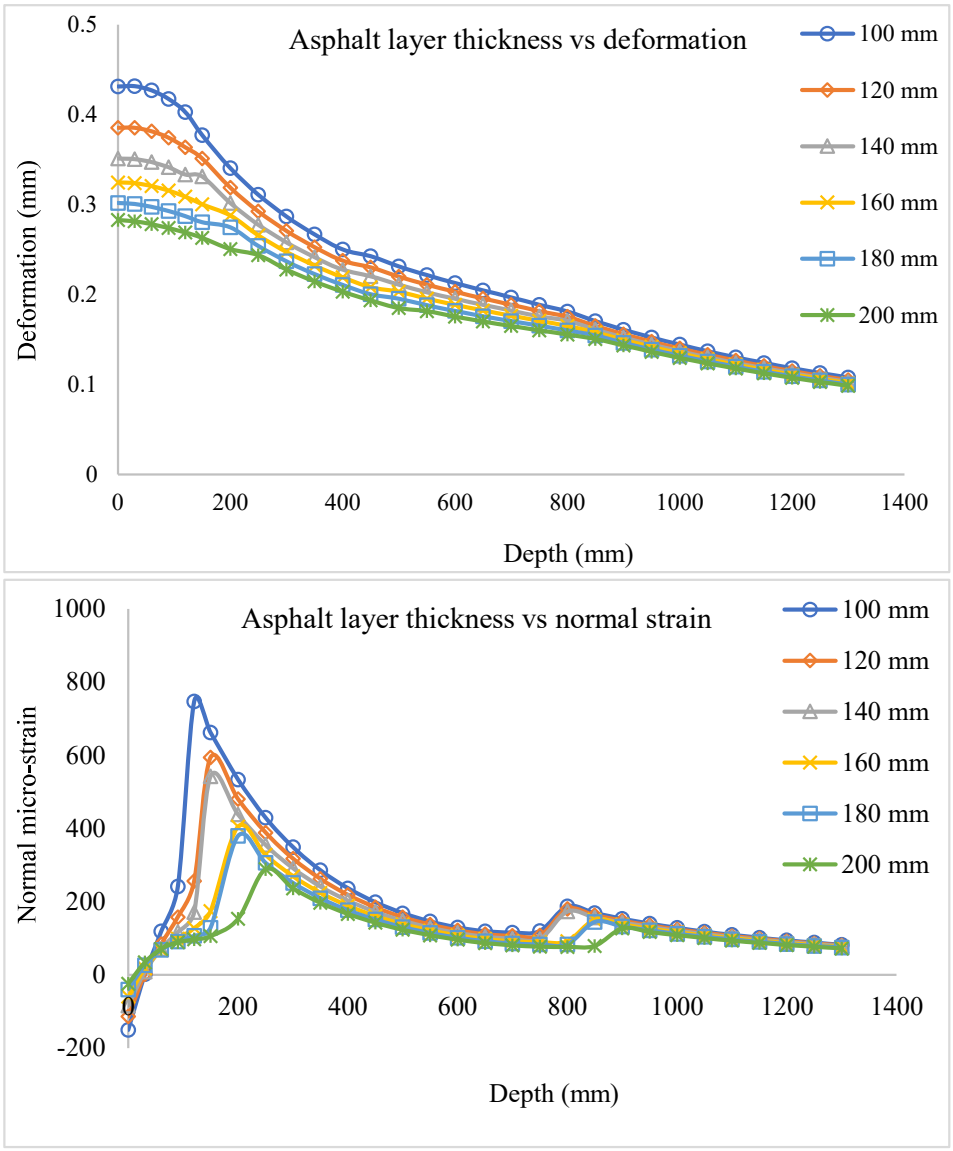

Figure 6.22. Effect of asphalt layer thickness on deformation and normal strain.

The thickness of each layer in asphalt pavement has huge role in controlling pavement response. The exact benefit in terms of percentage increase in pavement life has been reported in a few past studies considering linear elastic approach. This analysis provides a more realistic solution using LVE simulation. Firstly, effect of increase in asphalt layer thickness on vertical deformation and normal strain has been discussed followed by estimation of pavement life in rutting and fatigue. As shown in Figure 6.22, it was found

that maximum surface deformation decreases by 10.61, 18.56, 24.69, 30.02, and 34.41% respectively for every 20 mm increase in asphalt layer thickness from 100 mm to 200 mm. The above results show the significant effect of asphalt layer thickness in limiting surface deformation. This is important to note that, the percentage reduction in surface deformation is higher at lower asphalt thickness and gradually these decreases with increase in thickness. So, it can be concluded that, increase in asphalt layer thickness is more effective to control structural response when it is of lower thickness. Similar results were obtained in case of normal strain also. However, effect of increasing asphalt thickness on maximum compressive strain was more significant than in case of vertical deformation. For a similar increase in asphalt thickness of 20 mm from 100 mm to 200 mm, maximum compressive strain in the pavement was found to reduce by 20.95, 27.55, 45.75, 49.64, and 61.06% respectively. Although, these results correspond to maximum compressive strain in the pavement, it is not considered as critical parameters to define pavement life. Thus, critical mechanistic parameters (ε_z and ε_t) at specific locations as explained earlier were determined as shown in Figure 6.23 to further estimate subgrade rutting and asphalt fatigue life.

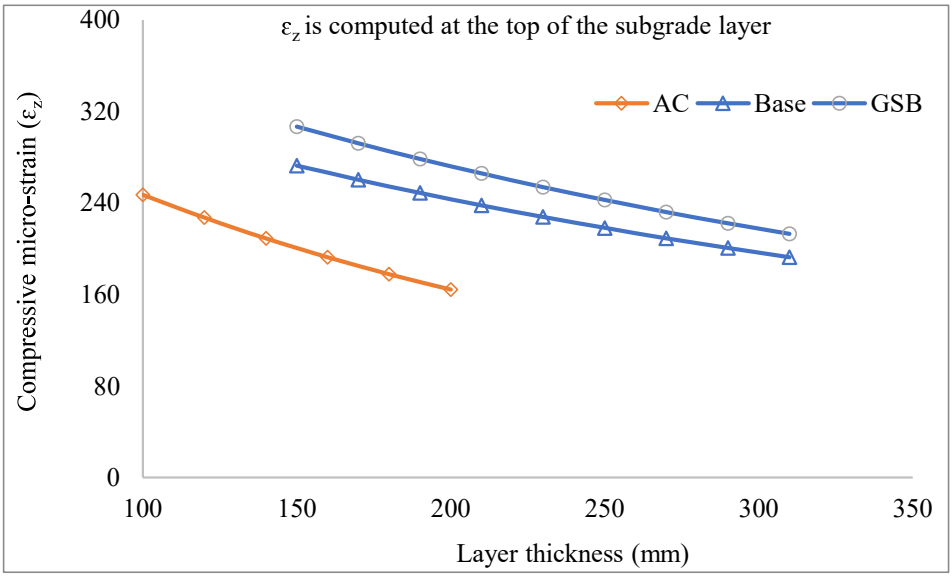

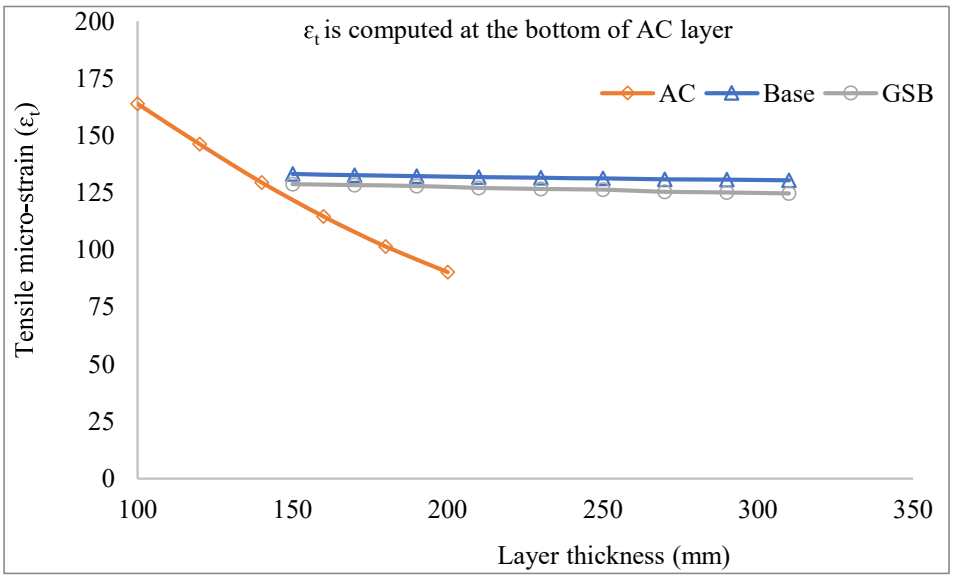

Figure 6.23. Effect of layer thickness on ε_z and ε_t under LVE simulations.

This is important to understand that, change in asphalt layer thickness has huge potential to limit compressive as well as tensile strain in the pavement. Figure 6.23 shows the possible reduction in ε_z and ε_t with the increase in asphalt layer thickness. It was found that, the increase in thickness has higher impact on tensile strain as compared to compressive strain. An average reduction of 7.82% in ε_z value was obtained for every 20 mm increase in asphalt layer thickness from 100 mm to 200 mm. However, with the similar changes, an average reduction of 11.23% in ε_t value was obtained. This shows the relative impact of asphalt thickness on ε_z and ε_t value. These are indicative parameters to pavement performance in rutting and fatigue. The other important finding to note that is, change in other lower layer's (base and subbase) thickness has very less effect on compressive strain while negligible effect on horizontal tensile strain. Since, ε_t is measured at the bottom of asphalt layer, so any change in lower layer's thickness practically makes no difference as expected. An average reduction of only 0.33% in ε_t was found for every 20 mm increase in either base or subbase layer thickness. However, for similar changes, effect on ε_z was found considerable. An average reduction of 4.36%

in ε_z was found for every 20 mm increase in base or subbase layer thickness from 150 mm to 310 mm.

It can be concluded that, to limit ε_z, cost-benefit analysis is required as all the layers have potential to reduce it significantly. However, to limit ε_t, the option of suitable change in asphalt layer thickness shall be selected. These strains were further used to estimate subgrade rutting and asphalt fatigue life as shown in Figure 6.24 to Figure 6.26.

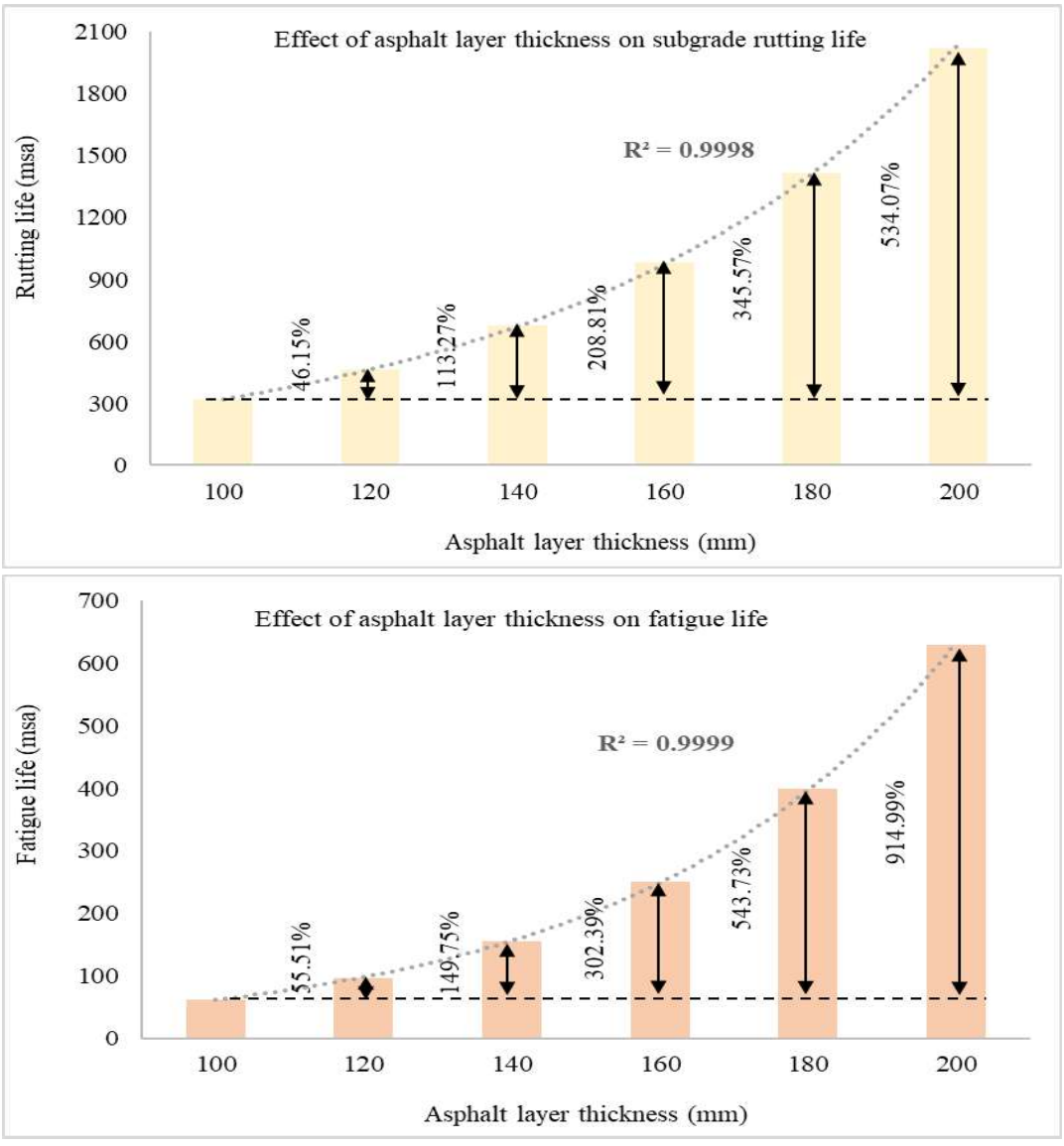

Figure 6.24. Effect of asphalt layer thickness on subgrade rutting and asphalt fatigue life.

This shall be noted that fatigue life of asphalt layer has been estimated using equivalent resilient modulus that could have produced similar tensile strain as in case of LVE simulations. Effect of change in asphalt layer thickness on subgrade rutting and asphalt fatigue life is shown in Figure 6.24. The exponential increase in subgrade rutting as well as asphalt fatigue life was obtained with the increase in asphalt thickness. All the changes in pavement life is presented in the form of percentage increase with respect to the minimum thickness selected as base line.

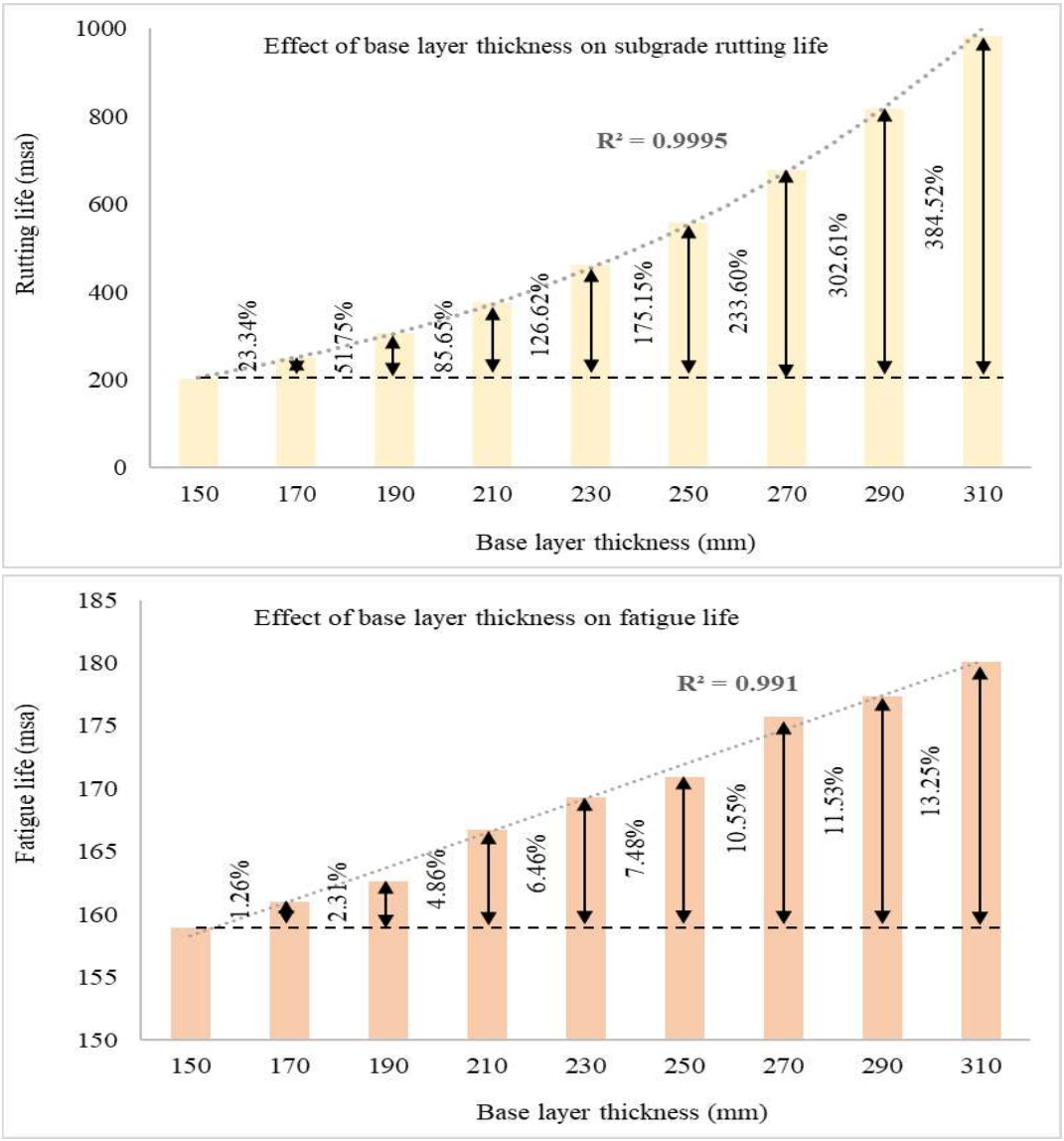

Figure 6.25. Effect of base layer thickness on subgrade rutting and asphalt fatigue life.

The higher impact on asphalt fatigue life can be seen in Figure 6.24 as it was also expected from the previous value of ε_t. The effect of base and subbase layer thickness on pavement performance in terms of subgrade rutting and asphalt fatigue life is shown in Figure 6.25 and Figure 6.26. The subgrade rutting life was found increasing exponentially with the increase in base layer thickness similar to that in case of asphalt layer while effect on asphalt fatigue life was found linear. The effect on rutting life is significant while for a small increase in asphalt fatigue life, considerable increase in base layer thickness is required. The effect of increase in subbase layer thickness on subgrade rutting and asphalt fatigue life is shown in Figure 6.26.

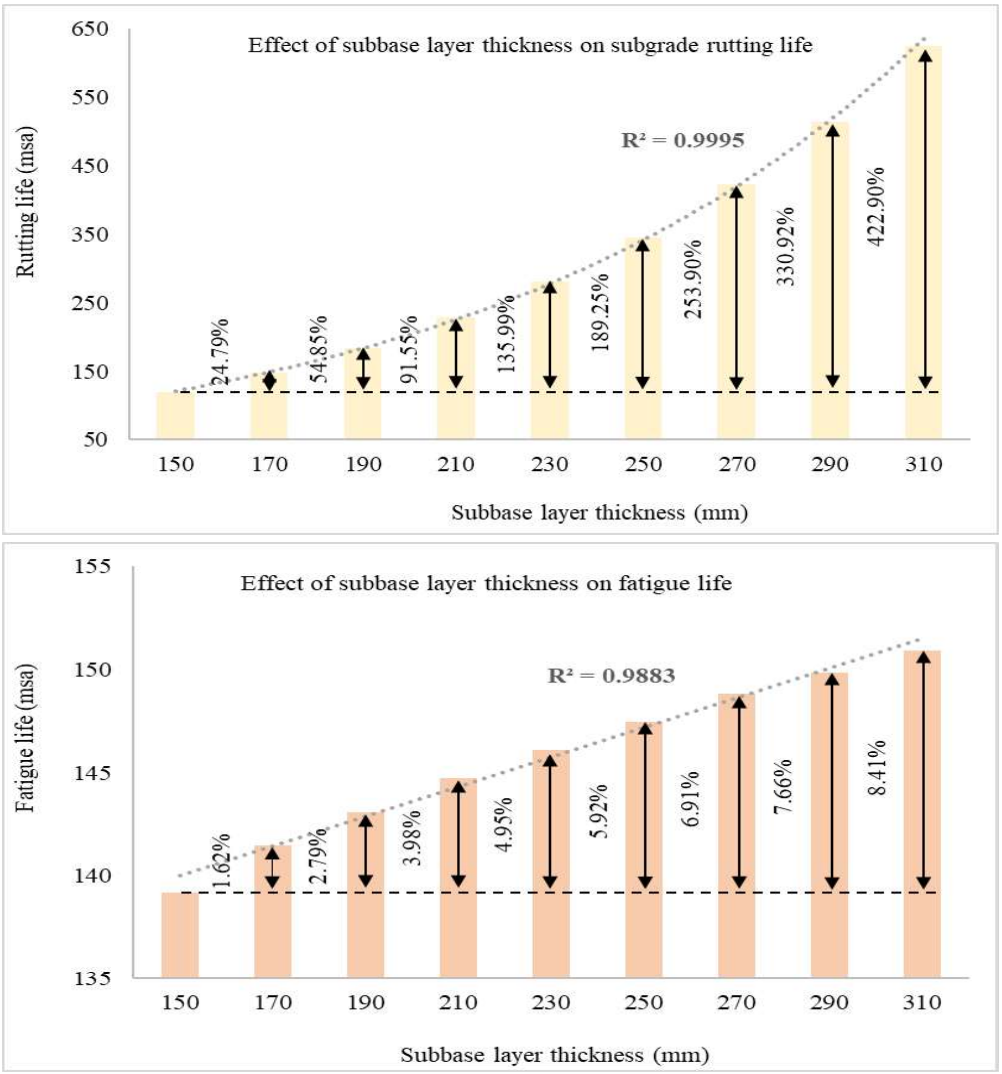

Figure 6.26. Effect of subbase layer thickness on subgrade rutting and asphalt fatigue life.

The effect of increase in subbase layer thickness on subgrade rutting and asphalt fatigue life is similar to that of base layer as increase in rutting life is exponential and fatigue life is linear with almost similar percentage increase. As shown in Figure 6.25 and Figure 6.26, it was found that, the subgrade rutting life increases by 384.52% for an increase of 160 mm of base layer thickness while it increases by 422.90% for the similar increase in subbase layer thickness. So, it can be concluded that, effect of subbase layer thickness has slightly higher impact on subgrade rutting. However, the same is not true in case of fatigue life performance. For similar increase in base and subbase layer thickness, asphalt fatigue life was found to increase by 13.25% and 8.41% respectively. Although, variation in these layer thicknesses has no significant effect on fatigue life; however, effect of base layer thickness has relatively higher impact.

6.5 Linear viscoelastic AC, stress dependent UGMs and nonuniform loading

This section of study considers LVE properties of AC, stress dependent behaviour of UGMs, and nonuniform loading conditions using real tire body. This analysis can be considered as more realistic simulation to field condition as compared to previous (stage I to stage III) simulations as it also considers nonlinear elastic behaviour of UGMs. The objective of analysis is to understand the effect of considering complex material properties of UGMs on the pavement response and its life (rutting and fatigue) under overloading conditions. Other parametric analyses (effect of temperature, layer thicknesses etc.) was not done to avoid repetition. Also, the effect of temperature is mainly visible in asphalt layer that has already been shown in stage II and stage III simulations.

6.5.1 Effect of loading

Standard load of 40 kN on single tire and overloading (with respect to 40 kN) of 25% to 100% has been considered to study the effect of loading on mechanistic response of the pavement and its life. The stress dependent behaviour of red soil (RS-1) for subgrade layer, GSB grade V, and WMM for base layer has been considered in this study while LVE response of BC-2 as asphalt layer has been chosen. Material properties of asphalt mixes and UGMs are discussed in Chapter 4 and Chapter 5 respectively. The effect of loading on mechanistic response and pavement life is shown in Figure 6.27.

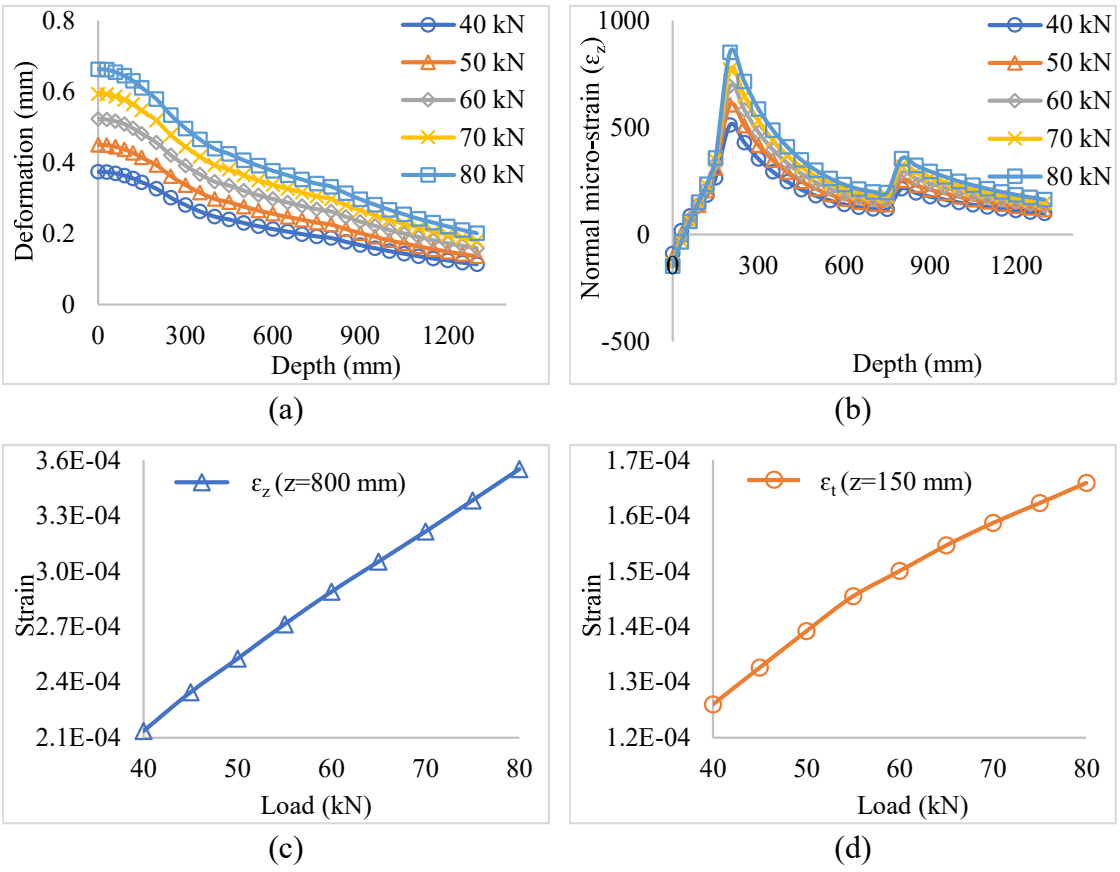

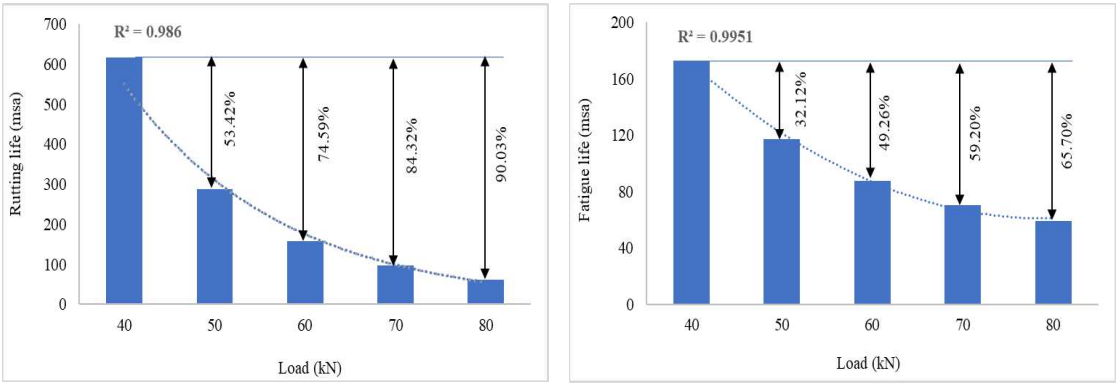

(e) (f)

Figure 6.27. Effect of loading on mechanistic response and pavement life.

As shown in Figure 6.27 (a), a 25% of overloading from 40 kN to 50 kN, increases maximum surface deformation by 20.24%. The damaging effect of overloading is similar to the previous cases (stage II and stage III simulations). However, it was found that when stress dependent behaviour of UGMs is considered, the obtained mechanistic response is slightly higher than when it is considered linear elastic. The variation in strain parameter as shown in Figure 6.27 (b)-(d) is also similar to the previous findings. The difference when compared with linear elastic solutions are shown in Figure 6.28. The rutting and fatigue life was found to decrease exponentially with the increase in loading as shown in Figure 6.27 (e)-(f). It was found that increase in loading has huge impact on pavement life as an increase in loading from 40 kN to 50 kN, reduces rutting life by 53.42% while fatigue life by 32.21%.

In this Chapter, it was shown that consideration of material behaviour in various layer has significant effect on the mechanistic response of asphalt pavement. In various stages of FE simulation, firstly linear elastic properties of the materials in various layers were considered followed by LVE asphalt layer and linear elastic UGMs, and in the final stage of simulation, LVE response of asphalt layer and stress dependent behaviour of UGMs were considered. The mechanistic response (maximum surface deformation and maximum normal strain) for this material behaviour has been summarised in Figure 6.28.

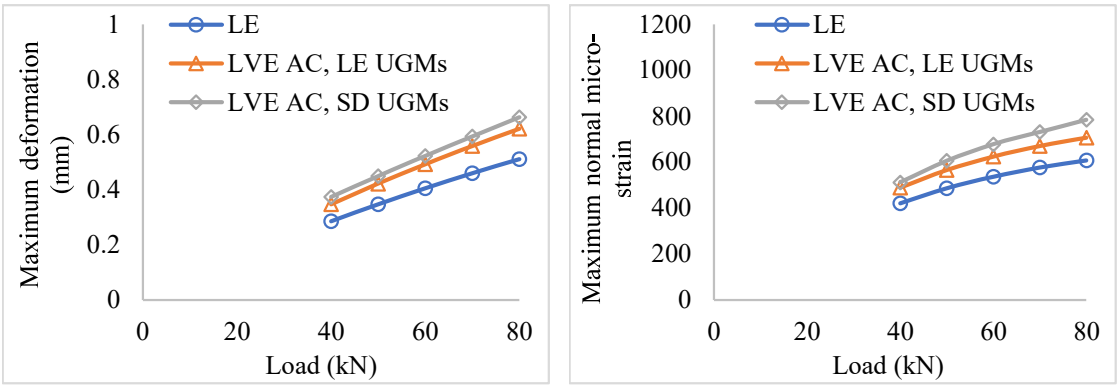

(a) (b)

Figure 6.28. Effect of loading on maximum (a) deformation and (b) normal strain.

Note: LE – material properties of all the layers were considered linear elastic

LVE AC, LE UGMs – LVE response of AC and linear elastic properties of UGMs

LVE AC, SD UGMs – LVE response of AC and stress dependent behaviour of UGMs

As shown in Figure 6.28 (a)-(b), the maximum surface deformation and normal strain were found highest when LVE asphalt and stress dependent behaviour of UGMs were considered. It can be concluded that, in case of static loading condition, linear elastic approach overestimates pavement strength and predicts lower mechanistic response.

6.6 Summary

This chapter covers parametric analysis of asphalt pavement using finite element method. The analysis has been categorized in four different stages of finite element simulation for ease of understanding and better clarity in technical discussions. Stage I simulation discusses effect of various loading shapes (circular, square, rectangular, and rectangle with semi-circular ends) on the structural response of asphalt pavement system considering linear elastic properties of materials in various layers of the pavement. The loading in this stage of FE simulation was assumed uniformly distributed over the contact area. The current pavement analysis and design methods in India are based on linear

elastic properties of the materials and uniform loading considering circular contact area. So, the idea of analysis was just to check whether shape of loading contact area makes any difference in the determination of pavement response or not. It was found that there is no significant effect of loading shapes on the structural response of asphalt pavement. However, rectangle with semi-circular shape results in lowest deformation and normal strain in the pavement while circular shape yields highest among all these shapes considered. The average difference in vertical deformation and normal strain considering these two shapes as obtained from FE analysis was found to be only 4.07% and 3.30% respectively. The rectangular and square shape yields similar results.

The stage II analysis considers linear elastic properties of materials in various layers and nonuniform loading using realistic solid tire. The FE model of solid tire body has been modelled in ABAQUS as discussed in Chapter 3. Tire has been modelled to simulate nonuniform contact stress distribution at tire-pavement interface. The parametric analysis was performed to study effect of key parameters (loading, type of asphalt mix, temperature, thickness of various layers, and stabilization of base layer) on the structural response and pavement life. The effect of loading on subgrade rutting life was found much higher than it has on asphalt fatigue life. An overloading of 25% (based on standard load of 40 kN on one tire) results in reduction of subgrade rutting life by 62.42% while fatigue life by 32.53%. The role of environmental factors like temperature also plays crucial role in deciding pavement performance. So, suitable selection of binder type and mix type for the construction of asphalt pavement is important and region specific. The analysis shows that, BC mixes are less sensitive than SMA mixes to change in pavement response at lower temperatures due to its dense gradation and thus higher stiffness. However, at higher temperatures, material properties of BC mixes are more sensitive to change in temperature as compared to SMA mixes which leads to significant increase in pavement

deformation and ε_z. The SMA mixes yields in relatively lower deformation and strains in pavement at higher temperatures; this is why SMA mixes are considered as rut resistant mixes at higher temperature and shall be used in high temperature regions.

When these parameters are not taken care of judiciously during design phase itself, higher stress and strains may result in early damage in asphalt pavement. These stress and strains can be limited by many ways. The conventional and straight forward approach pavement engineers generally go through is increase in layer thickness. The other way of thinking may be stabilization of base or subbase layer to increase layer stiffness which is gaining popularity over the years. However, large scale scientific data is required to prepare general guidelines for stabilization methods and warrants, its dosage, sampling techniques, and design criteria.

Looking into these challenges, both approaches (layer thickness and stabilization) were used to study its effect on pavement response and its life in terms of repetition of standard axle load. The effect of increase in asphalt layer thickness on asphalt fatigue life was found much higher than subgrade rutting life. Although, other lower layers have also potential effect in improving subgrade rutting life but lesser than asphalt layer. However, increase in base or subbase layer thickness has insignificant effect on fatigue life. So, it can be concluded that, ε_z can be limited by increasing thickness of any layer in the pavement and selection of a layer is based on cost-benefit analysis. The ε_t can be controlled significantly by increasing asphalt layer thickness only.

The other approach to limit these strains, stabilization technique was also considered in this analysis to study its relative effect on pavement response. In this study, base layer was treated with emulsion to stabilize it as discussed in Chapter 5. Firstly, vertical deformations, normal strains, ε_z, and ε_t were evaluated considering similar thickness of

conventional and stabilized base layer and it was found that emulsion treated base has huge potential in reducing these parameters. Further studies were carried out to see if these benefits can be utilized in reducing asphalt layer thickness. It was interesting to note that, the stabilized base layer can be used with 50 to 60 mm reduced asphalt thickness as compared to conventional base pavement system. It may result in cost saving as asphalt layer in the pavement is the costliest one; however, the cost of emulsion treatment needs to be carried out and require separate study. The benefit of emulsion treatment in terms of overloading leverage was also realized. Asphalt pavement in case of specified set of layer thickness and material properties was found to have 17.5 to 27.5% higher load carrying capacity in case of stabilized base layer than conventional base.

The stage III analysis considers LVE properties of asphalt mixes and nonuniform loading using realistic solid tire. Asphalt mixes are considered as viscoelastic material whose properties greatly varies with temperature and duration of loading. So, this analysis was carried out to study the effect of viscoelastic properties of asphalt mixes on pavement response and its life. This analysis may result in more realistic solution to asphalt pavement system. Similar parametric studies were carried out to study change in pavement response as compared to linear elastic approach.

The important finding from this simulation concludes, the LVE simulation was found to result in higher vertical deformation, normal strain, and ε_z at top of the subgrade layer while lower value of ε_t at bottom of the asphalt layer as compared to linear elastic simulation. For example, when standard load on single tire was varied from 40 kN to 80 kN at a difference of 10 kN (25%), LVE analysis resulted in 21.52% higher maximum deformation than linear elastic analysis. Similarly, for the same increase in loading, LVE analysis predicts 16.28% higher maximum compressive strain in the pavement and 15.94% higher ε_z at the top of the subgrade layer. However, for the similar changes in

loading, LVE solution yields in 25.43% lower ε_t at the bottom of asphalt layer. Similar trends were obtained for other parameters also. However, it shall be noted that, these results are based on static analysis only.

In the last stage of FE simulation, LVE response of asphalt layer and stress dependent behaviour of UGMs were considered and effect of loading on the mechanistic response of asphalt pavement were evaluated. The stiffness of the material considering tress dependent behaviour was found to reduce as compared to linear elastic consideration. This resulted in higher pavement response and lower rutting and fatigue life under increasing loading conditions. Based on static analysis results, it can be concluded that, linear elastic approach overestimates material stiffness and yields lower stress and strains in the pavement. Since, stiffness of the mix is higher in linear elastic analysis; so, ε_t is lower which results in lower asphalt fatigue life of the pavement. Based on the FE modelling of tire-pavement system (chapter 3), results obtained from material characterization of asphalt mixes (chapter 4), UGMs (chapter 5), and pavement analysis (in terms of structural response and pavement life) as discussed in chapter 6, the important conclusions and recommendations for future study has been highlighted in next chapter.